AGU ADVANCING EARTH AND SPACE SCIENCE

Water Resources Research

RESEARCH ARTICLE
10.1029/2021WR030874

Probabilistic Flood Hazard Mapping Considering Multiple Levee Breaches

A. Maranzoni[1], M. D'Oria[1], and M. Mazzoleni[2,3]

[1]Department of Engineering and Architecture, University of Parma, Parma, Italy, [2]Institute for Environmental Studies, Vrije Universiteit Amsterdam, Amsterdam, The Netherlands, [3]Centre of Natural Hazards and Disaster Science, Uppsala, Sweden

Key Points:

- A probabilistic method is presented for flood hazard mapping in flood-prone areas protected by levees, considering multiple breaches
- Breach scenario probabilities for selected return periods are estimated using levee fragility functions and basic probability rules
- A "central" hazard level map and an entropy index map are introduced to summarize probabilistic information on flood hazard

Correspondence to:
A. Maranzoni,
andrea.maranzoni@unipr.it

Citation:
Maranzoni, A., D'Oria, M., & Mazzoleni, M. (2022). Probabilistic flood hazard mapping considering multiple levee breaches. *Water Resources Research*, *58*, e2021WR030874. https://doi.org/10.1029/2021WR030874

Received 23 JUL 2021
Accepted 6 MAR 2022

Abstract Probabilistic methods are widely adopted for residual flood hazard assessment in flood-prone areas protected by levees. Such methods can consider various sources of uncertainty, including breach location and flood event characteristics, and allow for the quantification of the result confidence. However, the possible occurrence of multiple levee breaches during the same flood event is usually disregarded. This paper presents a probabilistic method based on levee fragility functions and basic probability rules to estimate the probability of selected breach scenarios, including multiple breaching events. The flood hazard classification is based on inundation variables calculated for flood events of different return periods. A combined 1D-2D hydrodynamic model is used for flood simulations. Probabilistic inundation extent maps and probabilistic flood hazard level maps are then created. Finally, probabilistic flood hazard estimates are summarized in a map of a suitable central tendency of the hazard level, coupled with a map of the Shannon entropy as an uncertainty indicator. This pair of statistical maps provides concise and effective information on a reference flood hazard along with the associated uncertainty. The method was applied to a region located along the middle reach of the Po River (northern Italy). Comparable central flood hazard estimates are obtained for the two sets of breaching events including or not including multiple breaches, with higher uncertainty if multiple breaches are considered. This result highlights the importance of considering multiple breaching events in flood risk management.

1. Introduction

Flood risk in floodplains has increased significantly in the last decades due to both climate change (Blöschl et al., 2019; Fang, 2016; Feyen et al., 2012; Ji et al., 2015; Kundzewicz et al., 2014) and anthropogenic processes (Hu et al., 2018; Mazzoleni et al., 2021; Viero et al., 2019). The potential damaging consequences of levee failures have been illustrated in numerous studies (e.g., Dierauer et al., 2012; Hui et al., 2016; Mohor et al., 2020; Orlandini et al., 2015; Sills et al., 2008). For example, Pistrika and Jonkman (2010) described the widespread damages caused in the residential New Orleans metropolitan area by the flooding resulting from the levee breaches that occurred during the 2005 destructive Hurricane Katrina, while Ferdous et al. (2019) documented catastrophic damages caused by the inundations due to levee breaches along the Jamuna River (Bangladesh) in the last decades.

Various structural and nonstructural measures have been widely developed and implemented to mitigate flood risk in urbanized floodplains and improve flood resilience. Among the nonstructural ones, early warning systems are topical, adaptive, and effective tools for flood risk reduction, since they allow flooding evolution to be efficiently predicted and emergency actions (such as evacuation of the exposed population) to be promptly activated (Alonso Vicario et al., 2020; Garcia & Fearnley, 2012; Mel et al., 2020). Classical structural measures, such as levee systems and flood retention basins, can also be adopted to provide protection of floodplain areas. In particular, levees ensure the protection of the surrounding floodplain areas by increasing the capacity and hydraulic conveyance of the river. However, the presence of levees does not completely eliminate the risk of inundation of flood-prone areas (e.g., Butera et al., 2020) and can even reduce flood risk awareness of communities living in the floodplains, producing the unintended effect of encouraging further urbanization, with consequent higher flood risk in the event of a levee failure (Akhter et al., 2021; Di Baldassarre et al., 2018; Hutton et al., 2019; White, 1945).

Flooding hazard assessment is crucial in the process of mitigating the potential catastrophic impacts of inundations caused by levee failures on flood-prone areas. Indeed, in flood risk analysis, flood hazard mapping is preparatory for consequence and loss estimation, emergency management, and land use and protection measure

planning (de Moel et al., 2009; EXCIMAP, 2007; FEMA, 2013, 2020; Klemešová, 2016; Merz et al., 2007), and in general is deeply involved in the definition of resilience strategies for flood risk management (de Bruijn, 2004; Karrasch et al., 2021). Various methods, both deterministic and probabilistic, have been proposed in the literature to quantify the residual flood hazard (Di Baldassarre et al., 2010).

The deterministic approach combines design hydrologic conditions with historical observations of breach characteristics, locations, and timing to empirically define a set of hypothetical scenarios based on selected inputs and parameter values (Aureli & Mignosa, 2004; Aureli et al., 2006; Ferrari et al., 2020; Kvočka et al., 2016; Shustikova et al., 2020; Urzică et al., 2021). In this deterministic context, the uncertainty in flood inundation predictions due to model inputs and parameters can be assessed by sensitivity analysis (Hall et al., 2005; Hesselink et al., 2003). The main advantage of this approach is that the results are direct and easily interpretable by decision-makers and stakeholders as well as conservative because they typically refer to the supposed "worst" scenario.

However, many sources of uncertainty, both aleatory and epistemic, potentially influence the accuracy of results (Beven et al., 2015; Dottori et al., 2013; Merwade et al., 2008; Pappenberger et al., 2006; Winter et al., 2018). For example, breach mechanism, location, size, geometry, and timing are highly dependent on the geometrical and geotechnical characteristics of the levee (Wahl, 2004), as well as on the severity of the flood event in the river. Probabilistic methods have been developed to take into account these uncertainties and provide valuable outcomes, such as inundation and hazard level probabilities (Apel et al., 2006; Most & Wehrung, 2005; Smemoe et al., 2007; Tyagunov et al., 2018; Vorogushyn et al., 2010, 2011). The characterization of the uncertainty is essential for a risk-based assessment in flood risk management processes (Hall et al., 2003; Harvey et al., 2014; Sayers et al., 2002). However, this additional information is usually obtained by stochastic Monte Carlo procedures, which are computationally expensive due to the large number of simulations needed, especially when flood hazard analysis involves wide floodable areas. Moreover, effectively communicating uncertainty in flood hazard assessments to stakeholders and decision-makers is not an easy task (Beven et al., 2015) and would require the use of meaningful and easy-to-read probabilistic maps.

Levee breach location is one of the uncertain factors that most influence flood hazard mapping. In the framework of probabilistic methods, Di Baldassarre et al. (2009) and Mazzoleni et al. (2014, 2017) computed probability-weighted hazard maps considering different flooding scenarios associated to overtopping- or piping-induced levee breaches characterized by different locations and geometric characteristics. D'Oria et al. (2019) proposed a probabilistic method based on the concept of levee fragility function and on the application of the probability multiplication rule to preselect single breach scenarios and calculate the associated probabilities for a design flood event of given return period. Recently, Curran, De Bruijn, Domeneghetti, et al. (2020) suggested a probabilistic approach that takes into account uncertainties in the levee fragility in a system behavior analysis for flood hazard assessment.

Regardless of the approach adopted, flood hazard mapping in flood-prone areas is typically performed assuming that levee failures may occur one at a time in a specific location. For example, Pinter (2005) modeled the residual flood hazard along the Upper Mississippi River assuming that a levee failure caused such a reduction in river stages as to prevent further levee breaches downstream. However, the occurrence of multiple levee breaches (i.e., breaches at different locations along the levee during the same flood event) is absolutely realistic. Indeed, during the 2005 Hurricane Katrina and the floods occurred in the Netherlands in 1993, multiple levee failures were recorded at different locations (Özer et al., 2020). Similarly, during the 2002 and 2013 flood events in Saxony and Saxony-Anhalt regions (Germany), multiple levee failures occurred (Thieken et al., 2016). Other examples of multiple levee failures concern the extreme flood events that mainly affected the Oder and Morava basins in the Czech Republic in 1997 (Özer et al., 2020), various historical floods affecting the Carpathian basin in Hungary (Bodi et al., 2014), and recent flood events in Italy (e.g., Viero et al., 2013). Nevertheless, the possibility of the occurrence of multiple levee breaches is usually overlooked in flood risk management (Jonkman et al., 2008), mainly because such high-order breach events are assumed to be very unlikely.

Few studies have dealt with the complex issue of probabilistic flood hazard mapping in the presence of multiple levee breaches. Dawson et al. (2005), Dawson and Hall (2006), and Harvey et al. (2014) proposed efficient techniques for flood risk analysis in floodplain areas protected by fluvial or coastal flood defense systems considering the failure (due to overflowing or breaching) of one or more components at selected sections. Apel

et al. (2006, 2009) analyzed the effect of the occurrence of a levee breach on the potential occurrence of further breaches downstream, based on probabilistic scenarios defined using levee fragility functions for overtopping. Courage et al. (2013) proposed a computational framework for flood risk management explicitly considering the system behavior (i.e., the modification of the flood wave due to a local levee failure). Ciullo et al. (2019) compared two flood risk management strategies in which river system behavior and hydraulic interactions are taken into account when multiple levee breaches occur. Bomers et al. (2019) explored the importance of levee breaches in influencing downstream flood risk and discharge partitioning in a bifurcating river system. Finally, a semi-probabilistic approach is reported in Curran, De Bruijn, and Kok (2020), in which hydraulic interactions are taken into account in multiple levee breaches deterministically triggered on the basis of water levels and water level duration.

Despite recent advances, a unified probabilistic approach that accounts for the uncertainty in both hydraulic load and multiple dependent breach positions is still missing. While previous studies have explored the effects of a probabilistic hydraulic loading in case of multiple independent levee breaches (e.g., Apel et al., 2006; Curran, De Bruijn, & Kok, 2020; Dawson et al., 2005), other studies have considered multiple dependent breaches in case of deterministic loading conditions (e.g., Ciullo et al., 2019). However, considering only one of these two aspects could lead to misleading flood hazard assessment and consequent flood risk. For these reasons, this study proposes a probabilistic method that combines the epistemic uncertainty on the location of multiple levee breaches with the aleatory uncertainty on the flood event, which is included considering flood events of different return periods. Specifically, the concept of levee fragility function and basic probability rules are used to preselect potential breach locations and identify a set of scenarios of multiple dependent levee breach locations with associated probabilities. A probabilistic inundation extent map and probabilistic flood hazard maps for given hazard levels are shown for a case study concerning a flood-prone area located on the right-hand side of the middle reach of the Po River (northern Italy). These maps are built on the basis of the inundation variables calculated using a combined 1D-2D shallow water hydrodynamic model.

The probabilistic hazard level information is summarized with a single "central" hazard level map coupled with an entropy index map representative of the uncertainty associated with the central estimate. The probabilistic maps obtained from two sets of breach scenarios — one formed only by single breaches and the other also including multiple breaches — are compared to assess the effect of multiple breach scenarios in flood hazard analysis.

2. Method

The probabilistic method presented in this paper extends the one recently proposed by D'Oria et al. (2019) by including multiple dependent breaches. The flowchart of the method is sketched in Figure 1.

Potential breach locations are preselected through a preliminary breach scenario analysis exploiting the probabilistic information provided by fragility functions of the discretized levee system. Single and multiple breaching events are identified using elementary combinatorics. Breach scenarios are then defined combining breaching events with selected flood events of different return periods. The probability of each scenario is calculated using basic probability rules. A 1D-2D shallow water model is used to simultaneously simulate flood propagation in the river (1-D model) and flooding in the flood-prone area (2-D model). Inundation and flood hazard maps for each breach scenario, associated with the corresponding probabilities, are finally processed to obtain probabilistic inundation and flood hazard maps.

The key elements and main assumptions of the method are the following.

1. Different breach locations characterize the potential breaching events, thereby taking into account epistemic uncertainty on breach location. Actually, the breach location is one of the factors that mainly affects the dynamics of a flooding resulting from a levee breach.
2. Levee reliability is described using fragility functions, which provide conditional failure probabilities for given river water stages at selected levee sections. Each individual section of the discretized levee system has a different resistance to flood loading and hence is characterized by a specific fragility function. Fragility functions for a given failure mechanism (piping) are considered in this paper as an example.

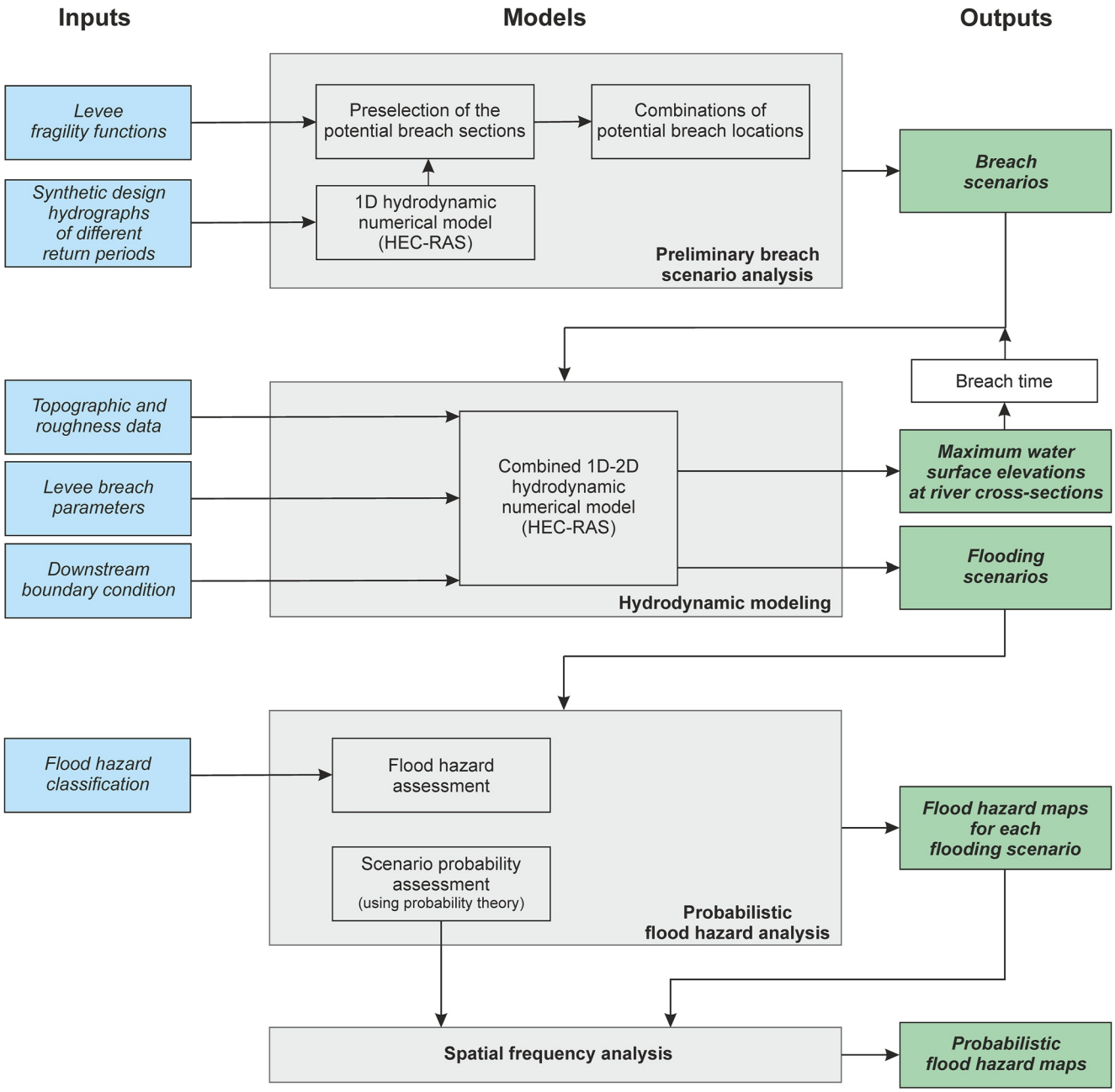

Figure 1. Flowchart of the probabilistic method.

3. The flood hazard classification adopted inherently incorporates the return period of the flood event. Accordingly, aleatory uncertainty on the loading flood event is taken into account considering synthetic inflow hydrographs with different return periods.
4. Except for the inflow boundary condition and breach location, all the other model inputs and parameters (topographic data, roughness coefficient in the river and in the floodable area, downstream boundary condition in the river, breach geometry and development) are treated deterministically and fixed a priori because this study focuses on uncertainty in flood event intensity and multiple breach locations on flood hazard assessment.
5. Multiple breach scenarios are considered, taking into account the effect of a breaching event on flood propagation and, consequently, on the probability that other breaches occur downstream.

6. The proposed probabilistic approach can also be applied when multiple levee breaches occur in both left- and right-hand side of the river channel. However, in the application shown in this study, we only consider the effect of the vulnerability of a one-side levee on the flooding hazard of the flood-prone areas.
7. The attainment of the peak flood level in the river triggers levee breaching at a specific section. Hence, breaches cannot occur at lower stages. Based on this hypothesis, the hydraulic load corresponding to the peak flow is assumed to be applied statically at each levee section, neglecting local unsteady effects associated with flood propagation. The effect of uncertainty in breach timing has been considered in D'Oria et al. (2019).
8. Due to the directionality of the flood propagation in the river and the inherent attenuation effect, the hydraulic load is applied sequentially to successive discrete levee sections from upstream to downstream. Therefore, in multiple breach scenarios, different breaches open sequentially from upstream to downstream during the same flood event. Breach opening in a certain location excludes that later a breach can open upstream.

The steps of the method are described in detail in the following subsections.

2.1. Preliminary Breach Scenario Analysis

The levee sections susceptible to failure are preselected based on the knowledge of the fragility functions of the discretized levee system.

The flood hazard classification is based on flooding variables concerning flood events of different return periods: 30, 100, and 200 years (see Section 2.3). Peak water levels at the cross sections used to discretize the river reach are predicted through a preliminary 1-D flood routing simulation of these three flood events. The potential breaches are located in those levee sections where a nonnegligible failure probability is computed for the less frequent flood event, even if the failure probability may be negligible or even zero for more frequent flood events. In this study, the failure probability is considered negligible if less than 0.015.

Once the potential breach locations are selected, elementary combinatorics is used to identify possible breaching events (defined in terms of location and number of breaches). Denoting the total number of preselected sections by N_{LS}, the possible breach scenarios are either $N_{LS}+1$ if only single breaches are considered or $\sum_{n=0}^{N_{LS}} C_{N_{LS},n} = 2^{N_{LS}}$ if multiple breaches are taken into account ($C_{N_{LS},n} = N_{LS}!/[n!(N_{LS}-n)!]$ being the combinations without repetitions of N_{LS} elements taken n at a time), including the no breach event in both cases (i.e., the event in which the levee withstands the flood loading without breaching).

To simplify the description of the method, N_{LS} is set to 4. However, the probabilistic approach can be extended to a higher value of N_{LS}, keeping in mind that if a long river reach is considered, the number of preselected breach locations (and consequently of potential breaching events) can be very large, making the analysis practically unfeasible. Limiting the application of the method to a relatively short river reach reduces the number of potential breaching events, allowing a detailed flood hazard analysis at a local scale.

Considering only single levee breaches, if $N_{LS}=4$, the space of the breaching events (Σ_1) is composed of events B_0, B_1, B_2, B_3, and B_4 (Figure 2a), where subscript "0" indicates the no breach event and subscripts "1", …, "4" refer to the levee sections breached (LS_1, LS_2, LS_3, and LS_4, respectively). If multiple breaches are taken into account, the following combinations can be identified: $C_{4,1}=4$, corresponding to four events with single breaches (B_1, B_2, B_3, and B_4); $C_{4,2}=6$, referring to six breaching events with two breaches (B_{12}, B_{13}, B_{14}, B_{23}, B_{24}, and B_{34}); $C_{4,3}=4$, concerning four events characterized by three breaches (B_{123}, B_{124}, B_{134}, and B_{234}); and $C_{4,4}=1$, since only one event presents four breaches (B_{1234}). The trivial no breach event (B_0) completes a set of $2^4=16$ combinations, which constitutes the space of breaching events (Σ_2) when multiple breaches are considered (Figure 2b). In Σ_2, multiple breaching events are $\sum_{n=2}^{N_{LS}} C_{N_{LS},n}$, which is equal to 11 for $N_{LS}=4$. In Figure 2b, Σ_2 is divided into $N_{LS}+1$ mutually exclusive subsets of breaching events. Subset $\boldsymbol{B}_1$ is composed of $\sum_{n=1}^{N_{LS}} C_{N_{LS}-1,n-1} = 2^{N_{LS}-1}$ events characterized by the occurrence of a breach at location LS_1. Subsets $\boldsymbol{B}_i \cap \bar{\boldsymbol{B}}_{i-1} \cap \ldots \cap \bar{\boldsymbol{B}}_1$ ($i=2, \ldots, N_{LS}$) are composed of $\sum_{n=i}^{N_{LS}} C_{N_{LS}-i,n-i} = 2^{N_{LS}-i}$ events characterized by a breach at LS_i and no breaches at the upstream sections LS_{i-1}, …, LS_1. The last subset consists of $2^{N_{LS}} - \sum_{i=1}^{N_{LS}} 2^{N_{LS}-i} = 1$ element, which is the no breach event.

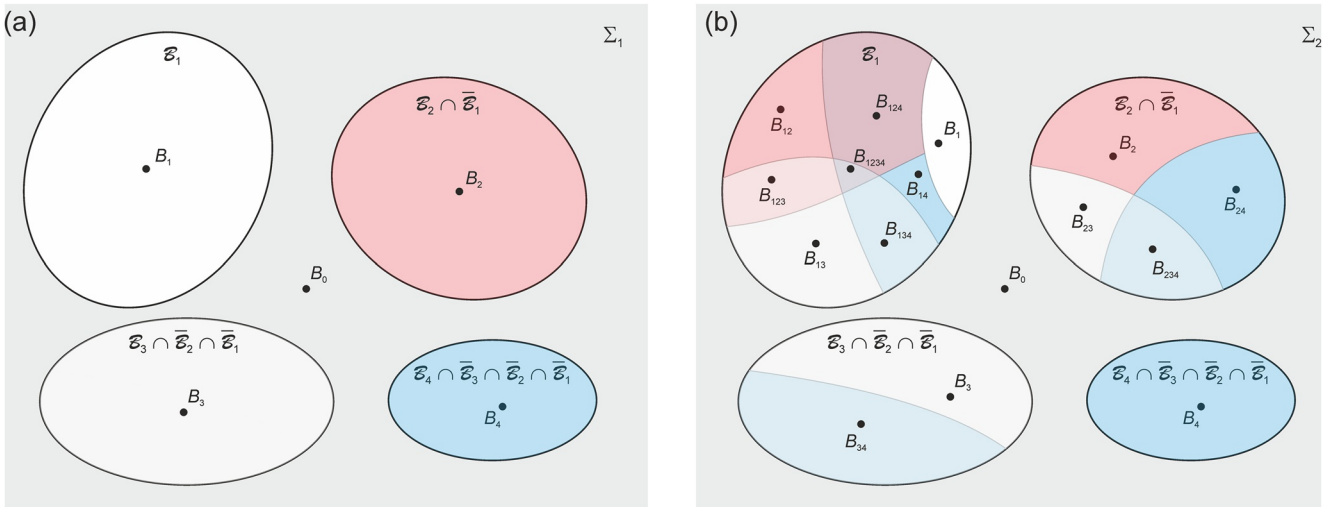

Figure 2. (a) Space Σ_1 of breaching events including only single breaches for four preselected breach locations ($N_{LS} = 4$). (b) Space Σ_2 of breaching events including multiple breaches for four preselected breach locations ($\boldsymbol{\mathcal{B}}_1$ is the space of breaching events with a breach at LS_1; $\boldsymbol{\mathcal{B}}_2 \cap \bar{\boldsymbol{\mathcal{B}}}_1$ is the space of breaching events with a breach at LS_2 but not at LS_1; $\boldsymbol{\mathcal{B}}_3 \cap \bar{\boldsymbol{\mathcal{B}}}_2 \cap \bar{\boldsymbol{\mathcal{B}}}_1$ is the space of breaching events with a breach at LS_3 but not at LS_1 and LS_2; $\boldsymbol{\mathcal{B}}_4 \cap \bar{\boldsymbol{\mathcal{B}}}_3 \cap \bar{\boldsymbol{\mathcal{B}}}_2 \cap \bar{\boldsymbol{\mathcal{B}}}_1$ is the space of breaching events with a breach at LS_4 but not at LS_1, LS_2 and LS_3; B_0 denotes the no breach event).

2.2. Hydrodynamic Model

The hydrodynamic model is the Hydrologic Engineering Center River Analysis System (HEC-RAS v. 5.07; Brunner, 2016a), developed by the U.S. Army Corps of Engineers. In particular, a combined 1D-2D model is used, in which the 1-D component simulates flood routing in the river solving the De Saint-Venant equations, while the 2-D component simulates the inundation dynamics in the flood-prone area (when one or more breaches occur) solving the full 2-D shallow water equations. The 2-D model takes advantage of an efficient subgrid approach (Brunner, 2016b), which allows the use of a relatively coarse computational grid without losing the detailed information of the underlying topography. Coupling between the 1-D and 2-D models is performed by means of lateral structures placed along the levee system, which models the flow exchange between the river and the adjacent floodable area according to a weir-type equation.

2.3. Flood Hazard Assessment

Flood hazard provides an overall quantification of the intensity and recurrence of a flooding and is usually expressed by a hazard level, which is evaluated through a classification based on suitable indexes (e.g., ACER, 1988; DEFRA, 2006). Hazard indexes are commonly defined as a function of one or more relevant flooding parameters, mainly maximum flood depth, maximum flow velocity, flood arrival time, rate of water depth rise, and flood duration. In most flood hazard analyses, flood hazard classification does not depend on the return period of the hydrologic event and hazard level estimates refer to a flood event of fixed recurrence interval (e.g., D'Oria et al., 2019; Mani et al., 2014; Mihu-Pintilie et al., 2019; Ongdas et al., 2020; Tingsanchali & Karim, 2005).

The flood hazard assessment method used in this study combines flooding intensity and flood recurrence. Differently from the method used by Aronica et al. (2012), which introduces distinct hazard level classifications for different selected return periods, this method defines hazard classes by setting specific thresholds on flood hazard indexes (namely maximum water depth and flow velocity) calculated for flooding scenarios of different return periods. The flood hazard level classification developed by the Adige River Basin Authority (northern Italy) and reported in Table 1 is implemented in this study. According to this classification, a hazard level is assigned to a flooded location if the corresponding condition is true, provided that the conditions relating to the higher hazard levels are not met. Five hazard levels (including the residual one) are defined in Table 1 on the basis of maximum values of water depth and flow velocity calculated for three flood events of different return periods (T = 30, 100, and 200 years). A unique flood hazard level can then be predicted for each breaching event, even though

Table 1
Flood Hazard Classification Adopted in This Study, Based on Flooding Variables Calculated for Different Return Periods

Condition	$h_{(T=200)}=0$	$h_{(T=200)}>0$	$h_{(T=100)}>0$	0.5 m $< h_{(T=30)} <$ 1 m or $h_{(T=100)} >$ 1 m or $v_{(T=100)} >$ 1 m/s	$h_{(T=30)} >$ 1 m or $v_{(T=30)} >$ 1 m/s
Flood hazard level	Residual	Low	Moderate	High	Very high
Flood hazard rating (*HR*)	0	1	2	3	4

Note. Flood hazard classification adopted by the Adige River Basin Authority (northern Italy), where h and v denote maximum values of water depth and flow velocity, respectively. T is the return period (in years). A flood hazard level (and the corresponding hazard rating [*HR*]) is assigned if at least one of the related conditions occurs and if, at the same time, the conditions reported in all columns on the right-hand side are not satisfied.

the analysis involves hydrologic events of different return periods. Moreover, inundations with equal hydraulic consequences resulting from more frequent hydrological events are classified as more hazardous.

2.4. Breach Scenario Probability Assessment

D'Oria et al. (2019) proposed a probabilistic method based on fragility functions and basic probability rules to estimate the probability of preselected breaching events conditioned to a design flood of fixed return period. However, this method neglects multiple breaches, assuming that the occurrence of a breach excludes the possibility that further breaches open downstream.

By applying the method of D'Oria et al. (2019) to a space of breaching events that neglect multiple breaches (Σ_1 in Figure 2a, which refers to the case of $N_{LS}=4$) and assuming that levee failure can only occur at the attainment of the peak water level ($\eta_{\max,T}$), the probability of breaching event B_i at the ith preselected levee section conditional to a design flood event of given return period T is

$$\begin{cases} P(B_i|T) = P_{f\,(LS_i)}(\eta_{\max,T}) & \text{if } i=1 \\ P(B_i|T) = P_{f\,(LS_i)}(\eta_{\max,T})[1-\sum_{k=1}^{i-1} P(B_k|T)] & \text{if } i=2,\ ...,\ N_{LS} \end{cases} \quad (1)$$

where probability $P_{f\,(LS_i)}$ provided by the fragility function for levee section LS_i must be considered a failure probability conditioned to the fact that no breaches have occurred before at any upstream preselected levee section. Accordingly, the probability of no breach event B_0 for a T-year return period flood event is

$$P(B_0|T) = 1 - \sum_{k=1}^{N_{LS}} P(B_k|T). \quad (2)$$

Breaching event probabilities must be considered conditional to a flood of fixed return period also when multiple breaches are taken into account (space of breaching events Σ_2 in Figure 5b). However, this specification is omitted in the following to lighten the notation. The meaning attributed to the fragility function probabilities yields

$$\begin{cases} P_{f\,(LS_i)}(\eta_{\max,\,B_0}) = P(\boldsymbol{\mathcal{B}}_i) & \text{if } i=1 \\ P_{f\,(LS_i)}(\eta_{\max,\,B_0}) = P(\boldsymbol{\mathcal{B}}_i|\bar{\boldsymbol{\mathcal{B}}}_{i-1}\cap\ldots\cap\bar{\boldsymbol{\mathcal{B}}}_1) & \text{if } i=2,\ldots,\ N_{LS} \end{cases} \quad (3)$$

where $\eta_{\max,\,B_0}$ is the peak water level calculated for the preliminary flood routing simulation in the absence of breaches (event B_0), $\boldsymbol{\mathcal{B}}_1$ is the space of breaching events in which a breach is present at LS_1, and $\boldsymbol{\mathcal{B}}_i|\bar{\boldsymbol{\mathcal{B}}}_{i-1}\cap\ldots\cap\bar{\boldsymbol{\mathcal{B}}}_1$ is the space of breaching events characterized by a breach at LS_i conditional on the fact that no other breaches have occurred at upstream sections LS_{i-1}, …, LS_1. The probabilities of each breaching event (conditional to a flood event of given return period) can then be calculated from elementary probability theory extending the method proposed by D'Oria et al. (2019). Calculations are detailed in Table A1 (Appendix A) for $N_{LS}=4$. The analysis can be easily generalized to different values of N_{LS}; however, it rapidly becomes complicated and laborious as N_{LS} increases.

The unconditional probability of each breaching event can be obtained by combining the conditional probability of the breaching events for a loading flood of given return period with the probability of occurrence of the flood events, according to the concept of compound probability of dependent events. In this analysis, rather than the annual probability $1/T$, the probability that a T-year return period flood event occurs at least once in a long-term period of N years is considered (Chow et al., 1988)

$$R_N(T) = 1 - \left(1 - \frac{1}{T}\right)^N. \tag{4}$$

This avoids having to handle extremely small probabilities, especially for high-order multiple breaching events. Since a discrete set of return periods T_j ($j = 1, \ldots, q$) is involved in the flood hazard level classification, the space of possible flood events is discretized with q flood events of selected return periods (in the flood hazard classification of Table 1, $q = 3$ and $T_1 = 30$ years, $T_2 = 100$ years, and $T_3 = 200$ years). On the basis of this discretization, a "weight" W_{N,T_j} is associated with each selected T_j-year return period flood event, representing the probability that a flood event equals or exceeds the T_j-year return period event without exceeding the T_{j+1}-one in a period of N years. Accordingly, for the case considered here ($q = 3$), the weights are

$$W_{N,T_1} = 1 - R_N(T_2), W_{N,T_2} = R_N(T_2) - R_N(T_3), W_{N,T_3} = R_N(T_3), \tag{5}$$

where W_{N,T_1} includes also the long-term probabilities of flood events with a recurrence interval lower than T_1. In this study, N is set to 200 years. Finally, the joint probability of a breaching scenario (defined as the combination of a breaching event B with a flood event of given return period T_j) in a period of N years is

$$P_N(B \cap T_j) = W_{N,T_j} \cdot P(B|T_j). \tag{6}$$

2.5. Probabilistic Mapping

Flood hazard maps are calculated independently for each breach scenario and associated with the corresponding probabilities. A flooding scenario probability analysis is then conducted, and the results are summarized in probabilistic flood inundation and hazard maps, as described in the following.

2.5.1. Probabilistic Inundation Extent Map

The probabilistic inundation extent map shows the probability of a given area to be flooded.

The inundation probability P_I at each floodable location $\mathbf{x}$ is calculated by adding the probabilities of the breach scenarios $B \cap T_j$ that induce flooding in $\mathbf{x}$, that is,

$$P_I(\mathbf{x}) = \sum_l P_N[(B \cap T_j)_l : h_{\max,l}(\mathbf{x}) > 0], \tag{7}$$

where $j = 1, \ldots, q$ refers to the different return periods considered, l is a counter of the breaching scenarios, and $h_{\max}$ is the maximum flood depth predicted by the hydrodynamic model.

2.5.2. Probabilistic Hazard Level Maps

Probabilistic hazard level maps provide the probability that a location in the floodable area is subject to a given flood hazard level (according to the hazard classification adopted) in a period of N years.

Since the return period of the flood event inherently contributes to the assessment of the hazard level according to the classification of Table 1, a unique flood hazard level is assigned to each location in the flood-prone area for a fixed breaching event. Accordingly, the total N-year probability (including all considered flood events with different recurrence interval) is attributed to each breaching event in probabilistic flood hazard mapping.

The spatial distribution of the probability of each hazard level is given by the sum of the total probabilities (with reference to a period of $N = 200$ years) of all breaching events B that determine a certain hazard level in each point $\mathbf{x}$ of the floodable area:

$$P_{HR=k}(\mathbf{x}) = \sum_l P_N[B_l : HR(\mathbf{x}) = k], \tag{8}$$

where HR is the flood hazard rating ($k = 0, \ldots, 4$ in the hazard classification of Table 1), which corresponds to a certain hazard level, and l is a counter of the breaching events. A discrete probability distribution of the flood hazard level is thus constructed for each location of the flood-prone area.

2.5.3. Probabilistic Hazard Level Design Maps

Two "statistical" maps are introduced to summarize the main characteristics of the probability distribution of the flood hazard level (considered as a discrete random variable) at each location potentially affected by flooding. These maps provide concise and essential information from the probabilistic hazard level maps and can be useful tools for design and decision-making purposes.

The first map represents the spatial distribution in the flood-prone area of the "expected" flood hazard level, quantified through a suitable central index of the flood hazard level variable. The median parameter (i.e., the flood hazard level expected to be exceeded with 50% probability in a period of 200 years) is chosen as the expected flood hazard level in this paper. The second map provides the spatial distribution of the uncertainty associated with the central estimate. This uncertainty is expressed here by the normalized Shannon entropy H', which is a variability index based only on probabilities (given the qualitative character of the random variable). It is defined as (Shannon, 1948; Singh, 2014)

$$H' = -\frac{1}{\ln N_{HL}} \sum_{k=0}^{N_{HL}-1} P_{HR=k} \ln P_{HR=k}, \tag{9}$$

where $P_{HR=k}$ denotes the probability of the kth hazard level (of hazard rating k) in a period of N years and N_{HL} is the total number of hazard levels considered (according to Table 1, $N_{HL} = 5$). If the probability of the kth hazard class is zero, the corresponding term $P_{HR=k} \ln P_{HR=k}$ in the sum appearing in Equation 9 must be set to zero because $\lim_{P \to 0^+} P \ln P = 0^-$. The normalized entropy index ranges from 0 to 1: it is equal to zero when the occurrence of a specific hazard level is certain (i.e., its probability is equal to unity), whereas it attains the maximum value of 1 when the variability of the probability distribution is maximum (i.e., all the hazard classes are equally probable). Therefore, values of H' close to zero indicate good reliability of the "expected" hazard level, whereas values close to unity indicate considerable uncertainty in the estimate of this design central parameter.

3. Case Study

The study area encompasses the middle reach of the Po River (northern Italy) between two consecutive right-hand side tributaries, the Taro and Parma Rivers (Figure 3). Along this 20 km river reach, a levee system protects highly anthropized areas on both river sides. Eleven surveyed cross sections are available for the description of the main channel, floodplains, and levees from the database of the Interregional Agency for the Po River (AIPo). Only the right-hand side levee is assumed to be susceptible to failure for simplicity, also because the historical breaching events documented in this reach of the Po River in the last 200 years mainly affected the right-hand side levee (Turitto et al., 2010). The levee breaches are assumed to be located just at the surveyed cross sections, where the geometry of the levees is known. The concept of fragility function is used to characterize the local reliability of the levee against a selected failure mechanism. The fragility functions for piping obtained by D'Oria et al. (2019) are used in this study since piping has been documented as the main cause of levee breaching in the middle reach of the Po River (Mazzoleni et al., 2015).

The river reach involved in the hydrodynamic simulations is 96 km long and extends up to the Cremona (upstream) and Borgoforte (downstream) gauging stations (Figure 3). Here, hydrological data are available to derive boundary conditions for the hydrodynamic model. The overall river reach is described by 61 surveyed cross sections (from the AIPo database) spaced approximately 1.6 km on average. A 2 m resolution digital terrain model (DTM) based on LiDAR data is also available for the entire area of interest.

If a breach occurs along the right-hand side levee of the Po River between the Taro and Parma tributaries, a 240 km^2 densely-urbanized and highly vulnerable area could be affected by flooding, extending from the right-hand side levee of the Taro River up to the left-hand side levee of the Enza River (Figure 3). This area is

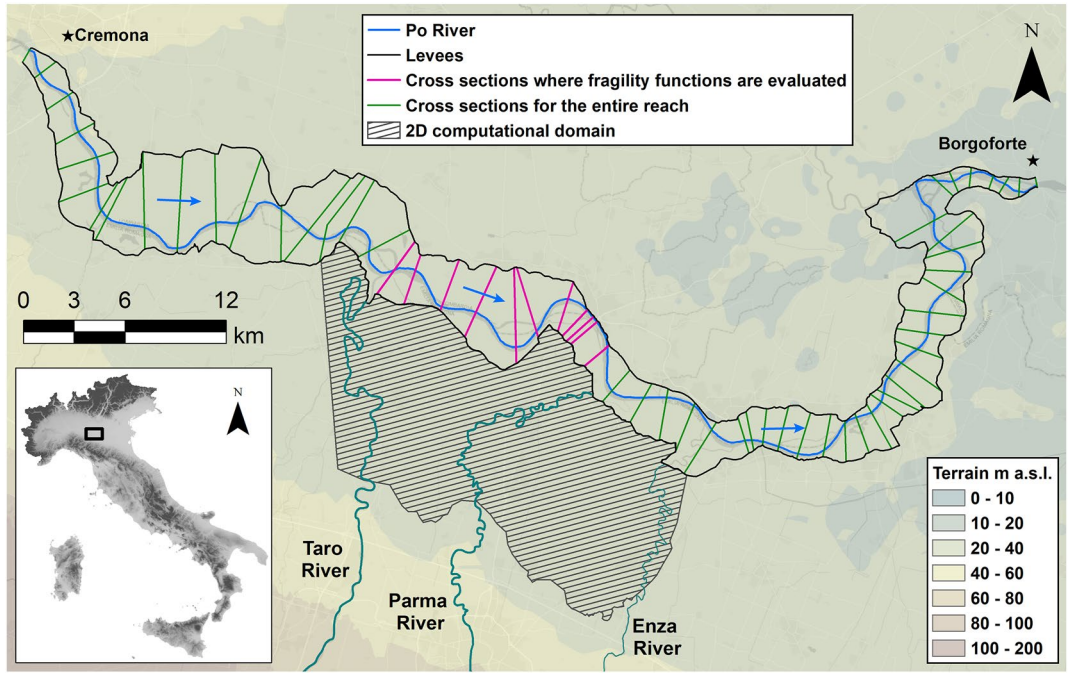

Figure 3. Reach of the Po River considered in this study. The right-hand side levee between the two tributaries Taro and Parma is assumed vulnerable to breaching. The river reach between Cremona and Borgoforte gauging stations is considered for flood routing modeling. The floodable area is delimited by the levees of the tributaries Taro and Enza.

subdivided into two distinct regions by the levees of the Parma River. In general, the levee systems of the main tributaries compartmentalize the flood-prone areas on the right-hand side of the middle reach of the Po River. This subdivision into compartments deeply influences the dynamics of flooding caused by a levee breach and can confine the inundation in the compartment where the breach has occurred or, at most, to immediately adjacent compartments. In this paper, the levee reliability analysis is limited to a relatively short levee stretch belonging to a single compartment and flood hazard assessment is performed only for the area potentially floodable as a result of breaching along this levee stretch. Since the method takes into account multiple breaches, this restriction reduces the total number of breach scenarios to consider avoiding a prohibitive computational effort.

In the 2-D model, the floodable area was discretized by a hybrid mesh composed of both structured and unstructured cells. To obtain this mesh, a preliminary structured mesh with a grid resolution of 30×30 m was built. The structured mesh was then locally refined using breaklines and unstructured cells to accurately reproduce the main barrier to flow (e.g., road embankments and levees), which can significantly affect the inundation process. The final mesh consists of 306,196 cells and 330,259 nodes.

In the 1-D model, two different values of the Manning roughness coefficient were set for the main channel and the floodplains along the Po River by calibration against hydrometric data measured during a severe historical flood event as described in D'Oria et al. (2019). In the 2-D computational domain, appropriate values of the Manning coefficient were selected (in the range 0.02–0.3 $m^{-1/3}s$) on the basis of land use (Corine Land Cover, 2012).

Synthetic design hydrographs with different return periods (30, 100, and 200 years) were calculated by the method proposed by Maione et al. (2003) and imposed at the upstream end of the 1-D model (Figure 4a), while a site-specific rating curve was specified as the downstream boundary condition (Figure 4b).

All breaches, regardless of their location, were assumed to be rectangular with a depth equal to the levee height (with reference to the landside ground level) and a fixed width of 100 m. This is an average value of historical

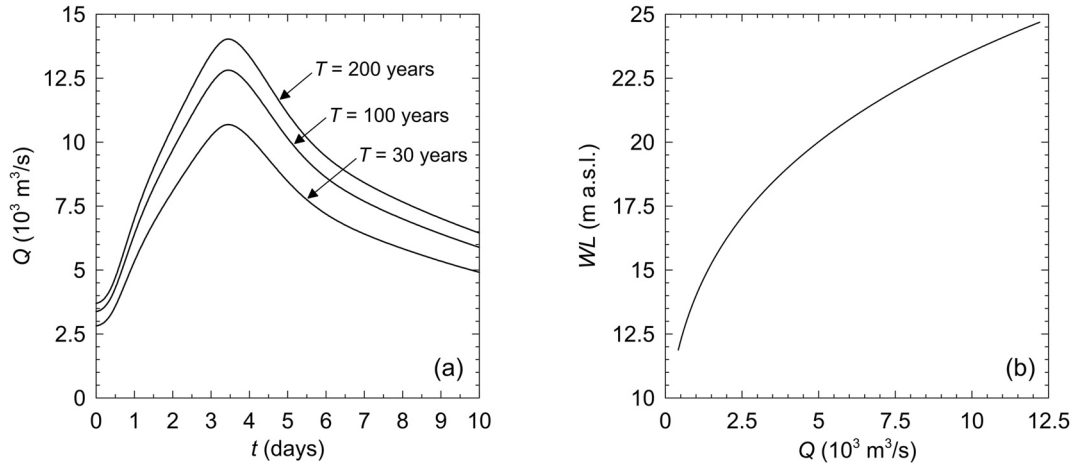

Figure 4. Boundary conditions of the hydrodynamic model: (a) inflow hydrographs for different return periods (T = 30, 100, and 200 years) at the Cremona gauging station and (b) rating curve at the Borgoforte gauging station.

breach width data concerning levee failures due to piping in the right-hand side levee of the considered river reach (Mazzoleni et al., 2015). Moreover, the levee failure was assumed to be instantaneous. The flow through the breaches was modeled using the standard weir equation, in which the dimensional weir coefficient was set to 1.1 $m^{1/2}s$ (Brunner, 2016a).

4. Results

4.1. Breach Scenarios and Associated Probabilities

Figure 5 shows the four preselected breach sections (LS_i, $i = 1, \ldots, N_{LS} = 4$) for the case study considered along with the corresponding fragility functions for piping obtained following D'Oria et al. (2019). Table 2 reports the conditional failure probabilities (P_f) derived from the fragility functions for the peak water levels calculated for the three flood events considered. It is worth noting that, at a fixed levee section, the failure probability increases with the return period of the flood. For the case study analyzed, failure probabilities are all zero for the 1-in-30 year flood and hence breaches are not expected along the levee during the passage of a flood with this recurrence.

The potential breaching events involving the four preselected breach sections are shown in Figure 2, either including or excluding multiple breaches.

The values of the "weights" defined in Equation 5 for the three flood events with different return periods (30, 100, and 200 years) are reported in Table 3 for $N = 200$ years. Finally, Tables 4 and 5 provide the breaching scenario probabilities P_N (in a period of $N = 200$ years) calculated for the two sets of events Σ_1 (including only single breaches) and Σ_2 (including multiple breaches), respectively, for the case study analyzed. The total probability of each breaching event, which is

$$P_N(B) = \sum_j W_{N,T_j} \cdot P(B|T_j), \tag{10}$$

is reported in the last row of the tables. The total probability of the multiple breaching scenarios is approximately 0.026 for the case study considered, while the total breach probability (i.e., the probability that at least a breach occurs) is approximately 0.218. The probability that no levee failures occur in a time period of $N = 200$ years is approximately 0.782 for both sets of breaching events Σ_1 and Σ_2. Scenario probabilities P_N reported in Tables 4 and 5 are considered as probabilities of the levee breach-induced flooding scenarios for probabilistic inundation and flood hazard mapping.

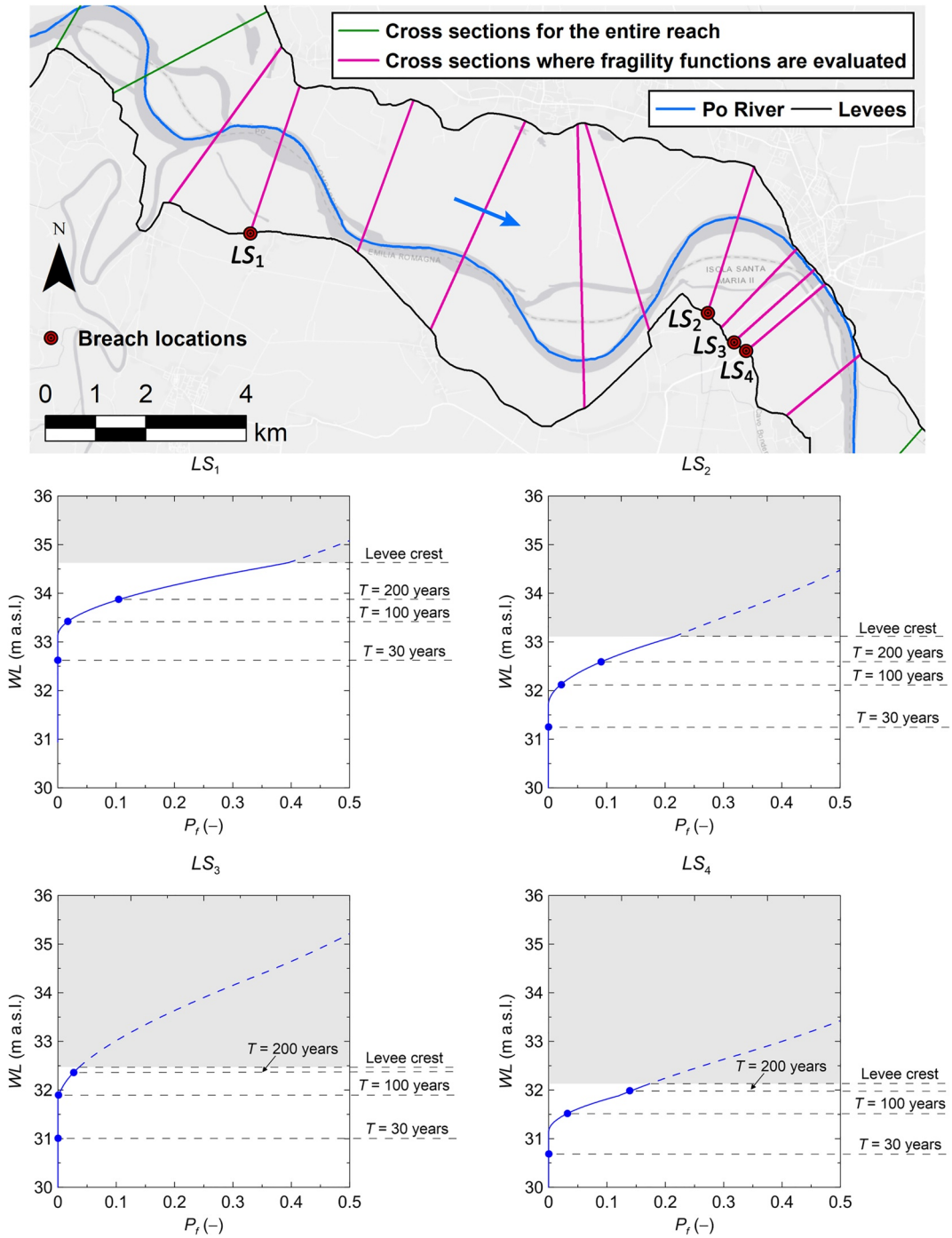

Figure 5. Preselected levee sections susceptible to failure (for piping) in the levee system considered and corresponding fragility functions.

Table 2
Conditional Failure Probabilities Obtained From Fragility Functions at Preselected Levee Sections for Three Flood Events of Different Return Periods

	P_f (−)			
T (years)	LS_1	LS_2	LS_3	LS_4
30	0	0	0	0
100	0.01841	0.02095	0.00139	0.03087
200	0.10456	0.09047	0.02764	0.14023

Note. Probabilities refer to the peak water level reached during the flood.

4.2. Probabilistic Inundation Extent Map

The first outcome of the flood hazard analysis is the probabilistic map of the inundation extent. Figure 6a shows the probabilistic inundation map obtained for the case study analyzed considering the complete set of breach events (which includes multiple breaches). The inundation probability reaches the maximum value of 0.218 in a large part of the flood-prone area. These zones are flooded for all breaching scenarios. On the other hand, probability values lower than 0.04 are observed in the south-eastern part of the flooded area. Abrupt changes in the inundation extent probability are caused by the secondary levee systems of the main right-hand bank tributaries of the Po River and by topographic obstacles that are barriers to flow.

The comparison of the probabilistic maps obtained with the two different sets of breach scenarios (including or excluding multiple breaches) allows to assess the effect of multiple breach scenarios on the predicted inundation probabilities. Figure 6b displays the differences between probabilistic inundation maps estimated with the complete set of breach scenarios (Σ_2) and the partial one (Σ_1), which does not include multiple breaches. Overall, the differences are small, and specifically no differences are found in most of the flood-prone area. This could be due to the flat topography of the region, which induces a rather uniform flooding in each compartment, masking the effect of multiple dependent breaches. However, in the south-eastern part of the flooded area, negative differences can be observed due to the higher values of the inundation probability calculated for the partial set of breaching events. Because of the compartmentation determined by the levees of the tributaries in the case study considered, inundations generated by multiple breach scenarios may mutually interfere producing a smaller flooded area. The complete set of breach scenarios provides higher inundation probabilities along the edges of the flooded area, especially in the south-western portion.

4.3. Probabilistic Hazard Level Maps

Figure 7 shows the probabilistic flood hazard maps for the study area for both the partial set Σ_1 and complete set Σ_2 of breaching events. Only four hazard levels appear in this figure ("high", $HR = 3$; "moderate", $HR = 2$; "low", $HR = 1$; and "residual", $HR = 0$) because the highest hazard level ("very high", $HR = 4$) does not occur in the case study analyzed. It is noteworthy that different hazard levels can occur in a specific location of the flood-prone area with different probabilities. This is a peculiarity that differentiates the proposed probabilistic method from the deterministic ones, in which a single hazard level is assessed for each location. The probabilities of the different hazard levels obviously sum to unity for each location.

For both Σ_1 and Σ_2 sets, the highest flood hazard levels occur close to the breach locations and tend to decrease far from them and the main levee. In the central part of the flood-prone area facing the three contiguous breaches, the probability of the "high" hazard level attains a maximum value of approximately 0.218 (Figures 7a and 7b), while the probabilities of the "moderate" and "low" hazard levels are equal to zero (Figures 7c–7f). Consequently, the probability of the residual level is approximately 0.782 (Figures 7g and 7h). This means that all breaching events induce the "high" hazard level in this area. On the other hand, the probability of the "residual" hazard level is higher than 0.782 in the zones where one or more breaching events do not cause inundation (Figures 7g and 7h).

Table 3
"Weights" of Selected Flood Events of Different Return Periods (30, 100, and 200 Years) Based on the Probability That a T-Year Return Period Event Occurs at Least Once in N = 200 Years

T (years)	$W_{N,T}$ (−)
30	0.13398
100	0.23298
200	0.63304

Figure 8 shows the maps of the differences between the probabilistic hazard level maps obtained using the complete set of breach events (Σ_2) and the partial one (Σ_1) for the four relevant hazard levels. Small differences can be observed. In particular, in the western portion of the study area (on the left-hand side of the Parma River), the differences in the hazard level probabilities range between −0.015 and +0.025 for all flood hazard levels. In this region, non-zero differences mainly occur at the boundaries of the flooded area. Non-zero differences affect a larger region in the eastern portion of the

Table 4
Estimated Probabilities of the Levee Breaching Scenarios in a Long-Term Period of N = 200 Years for the Space of Breaching Events Σ_1 (Including Only Single Breaches)

	$P_N(-)$				
Breach scenario	B_0	B_1	B_2	B_3	B_4
$T = 30$ years	0.13398	0	0	0	0
$T = 100$ years	0.21668	0.00429	0.00479	0.00031	0.00690
$T = 200$ years	0.43102	0.06620	0.05128	0.01425	0.07030
Total	0.78168	0.07049	0.05607	0.01456	0.07720

Note. The probability that a breach event occurs in a period of $N = 200$ years is 0.21832. The probability of the no breach event in a period of $N = 200$ years is 0.78168.

study area (on the right-hand side of the Parma River), with absolute values less than 0.025.

4.4. Probabilistic Hazard Level Design Maps

To derive the probabilistic design maps of the "expected" hazard level and the normalized Shannon entropy, the hazard level probability functions are calculated at each location excluding the no breach event B_0. Accordingly, the corresponding probabilities quantify the likelihood of given flood hazard levels, conditional to the occurrence of a breaching event. The hazard level statistics are then calculated on the basis of those events that induce flooding in the flood-prone area. Figure 9 shows an example of how the probability histogram of the flood hazard level variable changes at a selected location depending on whether the entire set Σ_2 of breaching events (including multiple breaches) or the reduced set $\Sigma_2 \backslash B_0$, which excludes the no breach event, is considered.

Figure 10 shows the map of the 50th-percentile hazard level coupled with the map of the normalized Shannon entropy for the case study considered. Both maps refer to the complete set of breaching events Σ_2, which includes multiple breaches. The two different sets of breaching events Σ_1 and Σ_2 provide almost the same median hazard level map. However, differences in the Shannon entropy maps can be observed in Figure 11. Therefore, for the case study analyzed, considering multiple breaching events does not induce substantial changes in the median hazard level map, but noticeably influences the associated uncertainty. Moreover, it can be noted that the same estimate of the median flood hazard level in distinct locations can be affected by different uncertainty. The "expected" hazard level map is similar to the deterministic flood hazard maps usually provided as a result of

Table 5
Estimated Probabilities of the Levee Breach Scenarios in a Long-Term Period of N = 200 Years for the Space of Breaching Events Σ_2 (Including Multiple Breaches)

	$P_N(-)$				
Breach scenario	B_0	B_1	B_2	B_3	B_4
$T = 30$ years	0.13398	0	0	0	0
$T = 100$ years	0.21668	0.00410	0.00465	0.00030	0.00690
$T = 200$ years	0.43102	0.05126	0.04298	0.01228	0.07030
Total	0.78168	0.05536	0.04763	0.01258	0.0772

	$P_N(-)$					
Breach scenario	B_{12}	B_{13}	B_{14}	B_{23}	B_{24}	B_{34}
$T = 30$ years	0	0	0	0	0	0
$T = 100$ years	0.00008	0	0.00010	0.00001	0.00014	0.00001
$T = 200$ years	0.00476	0.00133	0.00779	0.00122	0.00689	0.00197
Total	0.00484	0.00133	0.00789	0.00123	0.00703	0.00198

	$P_N(-)$				
Breach scenario	B_{123}	B_{124}	B_{134}	B_{234}	B_{1234}
$T = 30$ years	0	0	0	0	0
$T = 100$ years	0	0	0	0	0
$T = 200$ years	0.00012	0.00071	0.00020	0.00020	0.00002
Total	0.00012	0.00071	0.00020	0.00020	0.00002

Note. The probability that a single breach event occurs in a period of $N = 200$ years is 0.19277. The probability that a multiple breach event occurs in a period of $N = 200$ years is 0.02555. The probability that a breach event occurs in a period of $N = 200$ years is 0.21832. The probability of the no breach event in a period of $N = 200$ years is 0.78168.

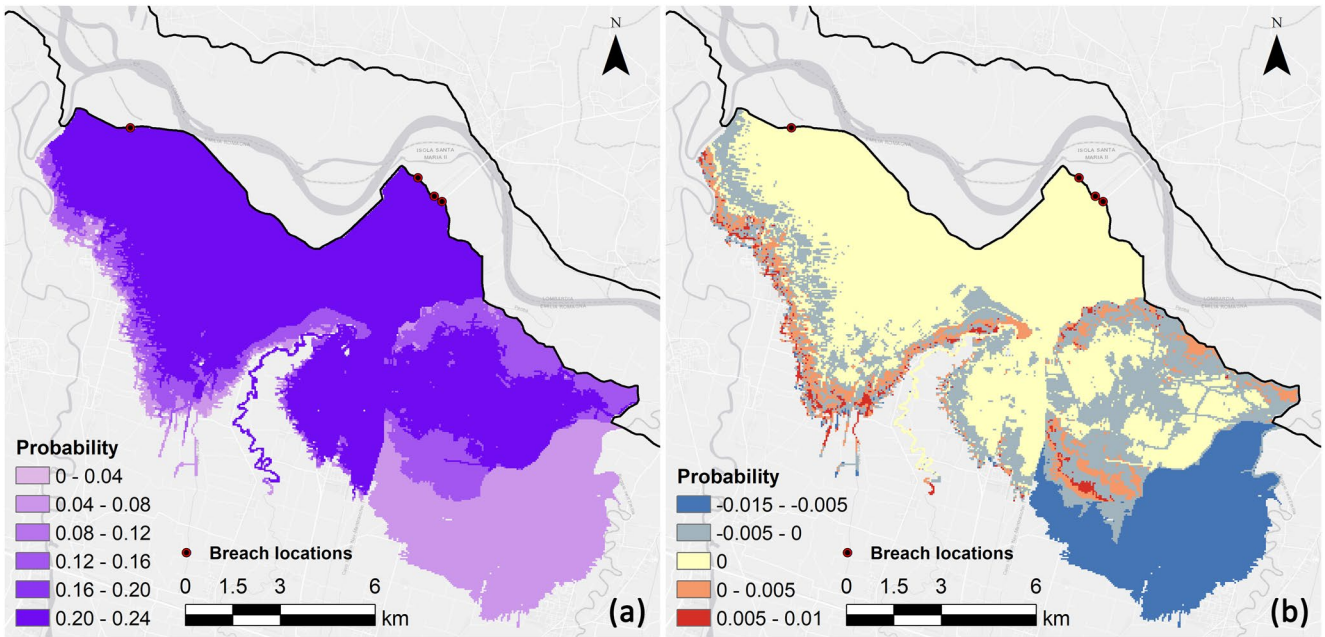

Figure 6. Probabilistic inundation extent maps (the probabilities indicated are 200-year probabilities). (a) Map obtained considering the complete set of breaching events (Σ_2) including multiple breaches. (b) Difference in estimated 200-year inundation probability between the complete set of breaching events (Σ_2) and the partial one (Σ_1) excluding multiple breaches.

conventional flood hazard analyses. However, the use of the probabilistic approach allows to add valuable information on the uncertainty in flood hazard level assessment.

An alternative "central" index of the hazard level probability distribution is the mode, which identifies the flood hazard level characterized by the highest probability. The contour map of the modal flood hazard level is shown in Figure 12a for the complete set of breaching events. A more precautionary prediction of the "expected" flood hazard level is provided by the map presented in Figure 12b, where the highest hazard level calculated at each location is shown, again for the complete set of breaching events. These maps can provide additional information useful to improve the robustness and informativeness of probabilistic flood hazard assessment in the area of interest to support flood-risk management actions and decision-making.

5. Conclusions

A probabilistic method is presented for flood hazard assessment in areas protected by levees that can be flooded in the event of a levee breach. The method generalizes the one by D'Oria et al. (2019) to the case of the occurrence of multiple breaches. Fragility functions at given levee sections are used to describe the reliability of the flood defense system against a selected failure mechanism and preselect the levee sections more susceptible to failure at the passage of a flood in the river, thereby including uncertainty on breach location in flood hazard analysis. In fact, breach location is one of the most significant factors that concur with the definition of the breach scenario and affect the delimitation of flooded areas and the appraisal of flood hazard.

The main novelties of this study are: (a) the fact that multiple breaching events (with dependent levee breaches) are taken into account, so that potentially very hazardous (albeit unlikely) inundation scenarios are included in the analysis; (b) the adoption of a flood hazard level classification in which the return period of the flood event is a relevant variable, so that uncertainty in flood intensity is also taken into account.

Once potential breach scenarios are identified (defined in terms of breach location and recurrence of the flood event), elementary probability theory allows unconditional probabilities to be assigned to each scenario. In this study, the unconditional probabilities are calculated for a long-term period (200 years) in order to obtain non negligible probabilities even for high-order multiple breaching events.

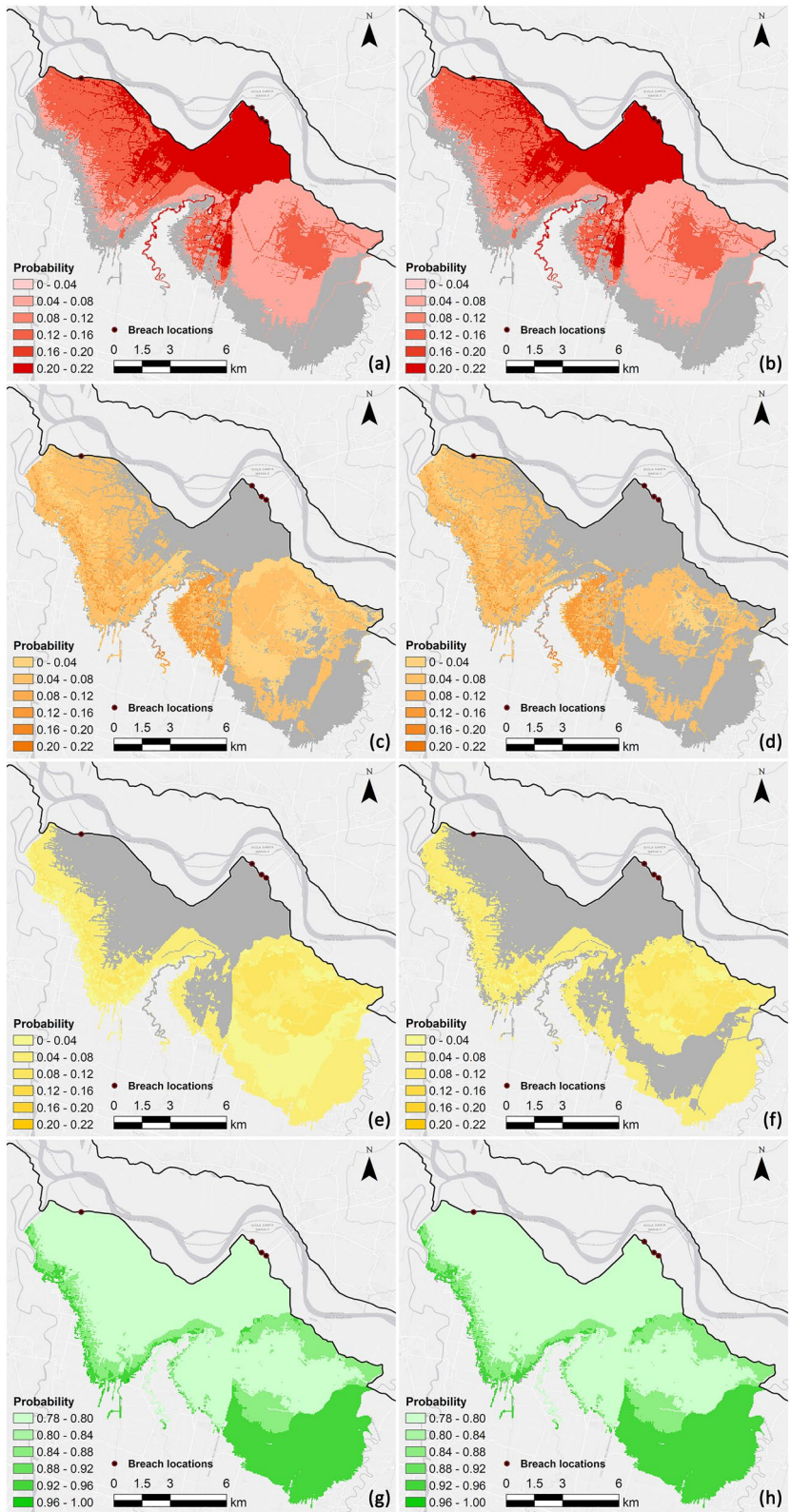

Figure 7. Probabilistic maps for four hazard levels according to the adopted classification: high (a and b); moderate (c and d); low (e and f); and residual (g and h). On the left-hand side, maps obtained considering the complete set of breaching events (Σ_2) including multiple breaches. On the right-hand side, maps obtained considering the partial set of breaching events (Σ_1) excluding multiple breaches. The probabilities indicated are 200-year probabilities. The heavy-gray background indicates the potential flooded area (i.e., the envelope of the inundation extents resulting from all breach scenarios).

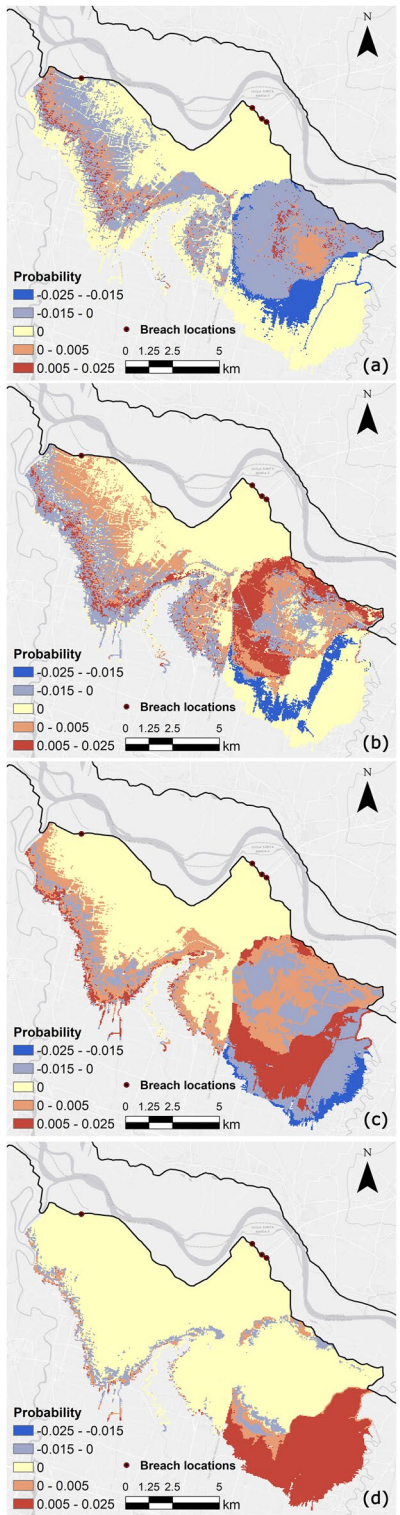

Figure 8. Difference in estimated 200-year probability of different hazard levels between the complete set of breaching events Σ_2 (including multiple breaches) and the partial one Σ_1 (including only single breach events): (a) high; (b) moderate; (c) low; and (d) residual.

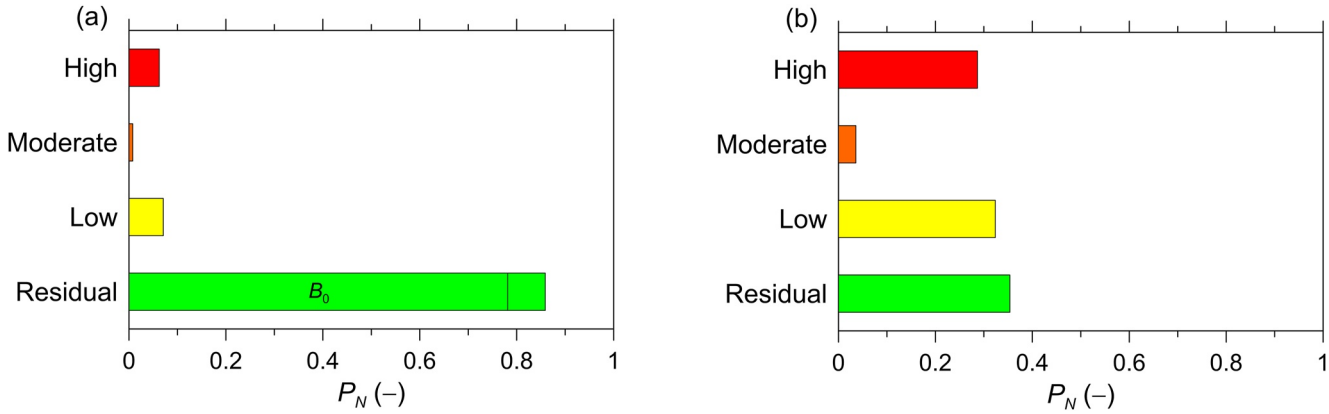

Figure 9. Flood hazard level probability histogram at a selected location based on (a) the entire breaching event set Σ_2 or (b) the reduced set $\Sigma_2 \backslash B_0$, which does not include the no breach event.

The method is applied to a flood-prone area located along the middle stretch of the Po River in northern Italy, focusing on a compartment delimited by the levees of two right-hand bank tributaries. The method is easily generalizable to other applications in different regions of the world, but the accuracy of the results is strictly connected with the quality of the input data, and in particular of the fragility functions of the levee system. In any case, an extensive application of the method to very long river stretches would become prohibitive due to the potentially large number of levee sections preselected as susceptible to failure and the consequent unmanageable number of breaching events. In this case, the calculation of breach scenario probabilities would become difficult and the hydrodynamic simulations computationally expensive, especially if a two-dimensional model is used on a high-resolution mesh to obtain an accurate description of the flooding in the flood-prone area.

The main outcomes of the method after spatial frequency analysis are the probabilistic inundation extent map and the probabilistic flood hazard level maps. The former shows the probability of each location in the floodable

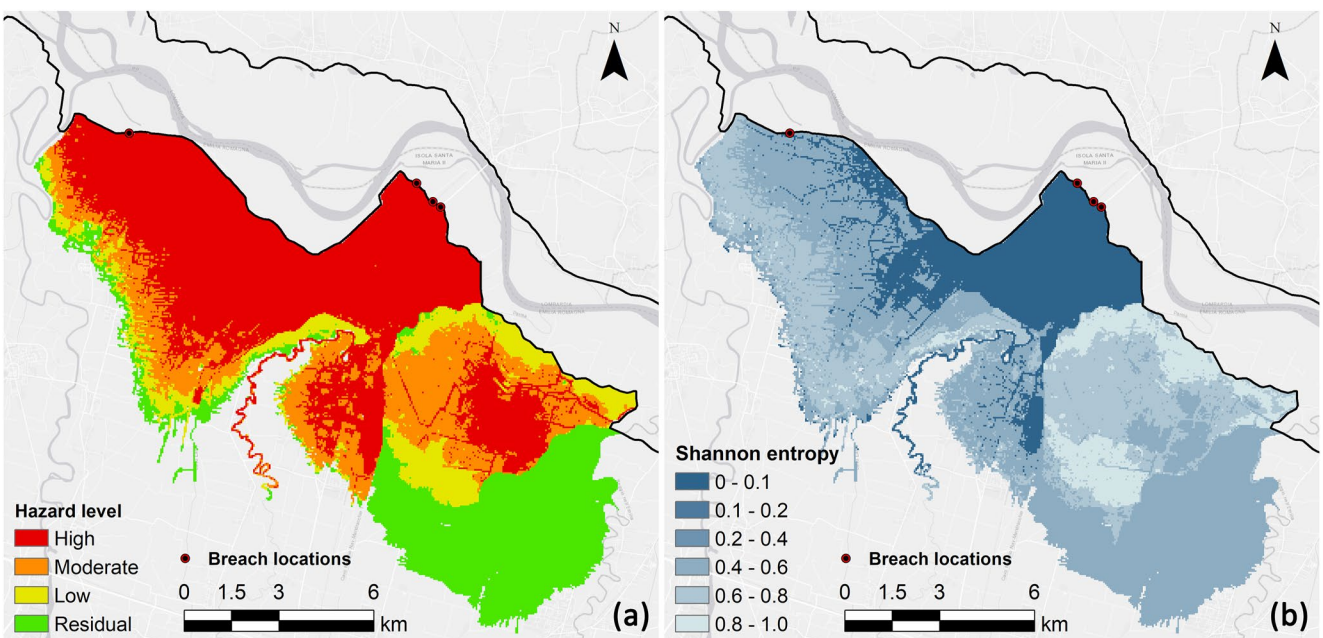

Figure 10. Probabilistic flood hazard maps for the complete set of breaching events (Σ_2): (a) 50th-percentile hazard level (excluding the no breach event), which is assumed as a design hazard level and (b) normalized Shannon entropy (ranging from 0 to 1), which is assumed as an estimate of the design hazard level uncertainty (values close to zero indicate good reliability of the design hazard level, whereas values close to unity indicate poor reliability).

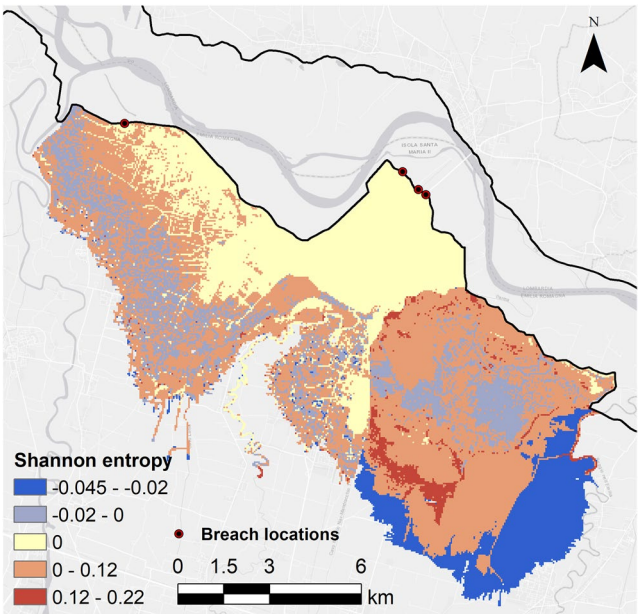

Figure 11. Difference in Shannon entropy between the complete set of breaching events Σ_2 (including multiple breaches) and the partial set Σ_1 (excluding multiple breach events).

area to be inundated. The latter maps provide the probability with which each distinct flood hazard level (defined according to a selected flood hazard classification) can occur in each location. Compared to the conventional deterministic flood hazard maps, the probabilistic ones contain richer information and support a more informed and effective identification of exposed infrastructure and population-at-risk sites requiring protective and flood mitigation measures, as well as warning and evacuation planning.

However, probabilistic flood hazard data cannot be exhaustively represented in a single map of practical and immediate use by decision-makers. To overcome this limitation, coupling the map of an "expected" hazard level (quantified through a suitable central index of the flood hazard level, considered as a stochastic variable) with the map of an uncertainty index (such as the normalized Shannon entropy) is proposed in this paper. This allows to condense the available probabilistic flood hazard information into just two statistical maps and provides a concise and effective idea about the spatial distribution of a "design" flood hazard along with the associated uncertainty. The representation of the results through an expected value along with the associated uncertainty is indeed sufficiently concise and easily interpretable and represents a possible improved way of communicating the results of a flood hazard analysis. Furthermore, this pair of maps can help to identify priorities in planning strategies, also based on the propensity to risk of the exposed areas (for example, investing economic resources primarily in the areas where highest flood hazard levels occur with the lowest uncertainty).

The comparison of the probabilistic maps obtained on the basis of the two sets of breaching events, including or not including multiple breaches, allows assessing the contribution of multiple breach scenarios on the predicted flood hazard. For the case study analyzed, taking into account multiple breaches does not induce substantial changes in the map of the median hazard level but noticeably influences the associated uncertainty, which increases if multiple breaches are considered.

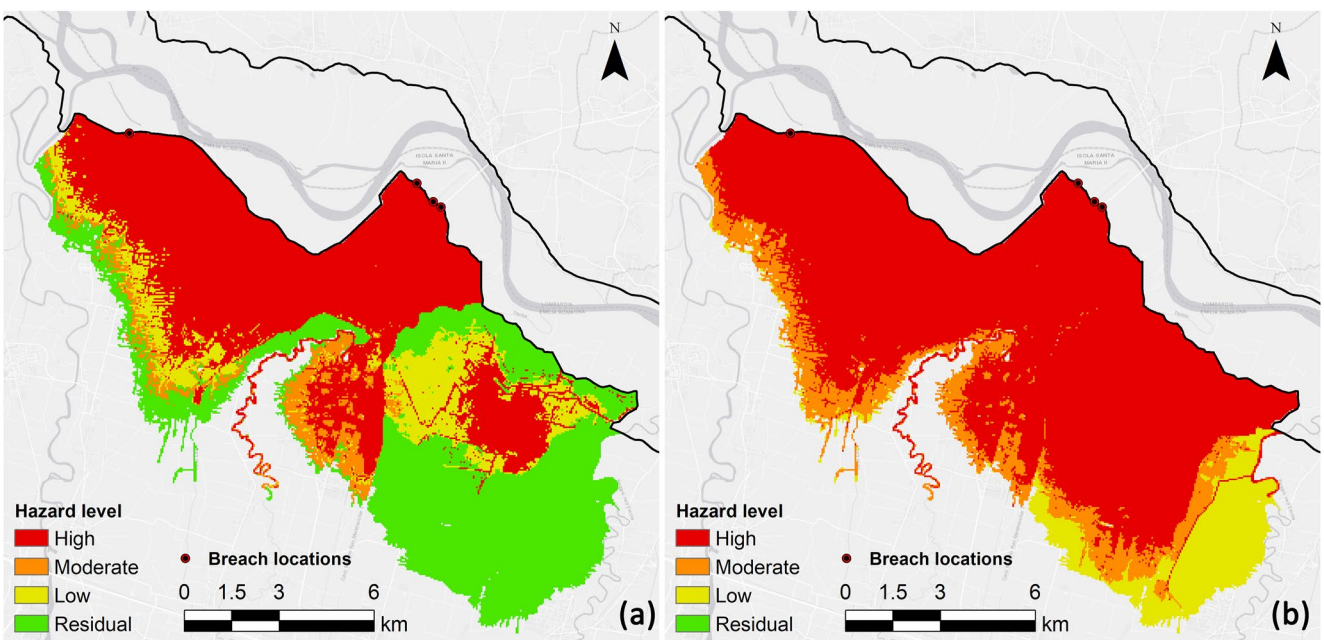

Figure 12. Maps of (a) the modal flood hazard level and (b) the maximum hazard level for the complete set of breaching events Σ_2 (including multiple breaches).

Appendix A: Table A1

Table A1
Calculations for the Assessment of the Probabilities (Conditional to a Flood Event of Given Return Period) of Breaching Events Belonging to Space Σ_2 Including Multiple Breaches ($N_{LS} = 4$)

Step no.	Preliminary knowledge	Breaching events	Adopted tool	Probability calculation	Description
1	Maximum water level at LS_1 from the preliminary flood routing simulation	$\mathcal{B}_1$	Fragility function of LS_1	$P(\mathcal{B}_1) = P_{f(LS_1)}\left(\eta_{\max,B_0}\right) = P(B_1 \cup B_{12} \cup B_{13} \cup B_{14} \cup B_{123} \cup B_{124} \cup B_{134} \cup B_{1234})$	Total probability of all breaching events including a breach at LS_1
2	Maximum water level at LS_2 from the flood routing simulation of breaching event B_1	$\mathcal{B}_2\|\mathcal{B}_1$	Fragility function of LS_2	$P(\mathcal{B}_2\|\mathcal{B}_1) = P_{f(LS_2)}\left(\eta_{\max,B_1}\right)$	Probability of all breaching events including a breach at LS_2 conditional to the occurrence of a breach at LS_1
3	Probabilities $P(\mathcal{B}_1)$ and $P(\mathcal{B}_2\|\mathcal{B}_1)$ from Steps 1 and 2	$\mathcal{B}_1 \cap \mathcal{B}_2$	Probability multiplication rule for dependent events	$P(\mathcal{B}_1 \cap \mathcal{B}_2) = P(\mathcal{B}_1) \cdot P(\mathcal{B}_2\|\mathcal{B}_1) = P(B_{12} \cup B_{123} \cup B_{124} \cup B_{1234})$	Total probability of all breaching events including breaches at LS_1 and LS_2
4	Maximum water level at LS_3 from the flood routing simulation of breaching event B_{12}	$\mathcal{B}_3\|(\mathcal{B}_1 \cap \mathcal{B}_2)$	Fragility function of LS_3	$P(\mathcal{B}_3\|\mathcal{B}_1 \cap \mathcal{B}_2) = P_{f(LS_3)}\left(\eta_{\max,B_{12}}\right)$	Probability of all breaching events including a breach at LS_3 conditional to the occurrence of breaches at LS_1 and LS_2
5	Probabilities $P(\mathcal{B}_1 \cap \mathcal{B}_2)$ and $P(\mathcal{B}_3\|\mathcal{B}_1 \cap \mathcal{B}_2)$ from Steps 3 and 4	$\mathcal{B}_1 \cap \mathcal{B}_2 \cap \mathcal{B}_3$	Probability multiplication rule for dependent events	$P(\mathcal{B}_1 \cap \mathcal{B}_2 \cap \mathcal{B}_3) = P(\mathcal{B}_1 \cap \mathcal{B}_2) \cdot P(\mathcal{B}_3\|\mathcal{B}_1 \cap \mathcal{B}_2) = P(B_{123} \cup B_{1234})$	Total probability of all breaching events including breaches at LS_1, LS_2, and LS_3
6	Maximum water level at LS_4 from the flood routing simulation of breaching event B_{123}	$\mathcal{B}_4\|(\mathcal{B}_1 \cap \mathcal{B}_2 \cap \mathcal{B}_3)$	Fragility function of LS_4	$P(\mathcal{B}_4\|\mathcal{B}_1 \cap \mathcal{B}_2 \cap \mathcal{B}_3) = P_{f(LS_4)}\left(\eta_{\max,B_{123}}\right)$	Probability of all breaching events including a breach at LS_4 conditional to the occurrence of breaches at LS_1, LS_2, and LS_3
7	Probabilities $P(\mathcal{B}_1 \cap \mathcal{B}_2 \cap \mathcal{B}_3)$ and $P(\mathcal{B}_4\|\mathcal{B}_1 \cap \mathcal{B}_2 \cap \mathcal{B}_3)$ from Steps 5 and 6	$\mathcal{B}_1 \cap \mathcal{B}_2 \cap \mathcal{B}_3 \cap \mathcal{B}_4$	Probability multiplication rule for dependent events	$P(\mathcal{B}_1 \cap \mathcal{B}_2 \cap \mathcal{B}_3 \cap \mathcal{B}_4) = P(\mathcal{B}_1 \cap \mathcal{B}_2 \cap \mathcal{B}_3) \cdot P(\mathcal{B}_4\|\mathcal{B}_1 \cap \mathcal{B}_2 \cap \mathcal{B}_3) = P(B_{1234})$	Probability of breaching event B_{1234}
8	Probabilities $P(\mathcal{B}_1 \cap \mathcal{B}_2 \cap \mathcal{B}_3)$ and $P(\mathcal{B}_1 \cap \mathcal{B}_2 \cap \mathcal{B}_3 \cap \mathcal{B}_4)$ from Steps 5 and 7	$(\mathcal{B}_1 \cap \mathcal{B}_2 \cap \mathcal{B}_3) \setminus (\mathcal{B}_1 \cap \mathcal{B}_2 \cap \mathcal{B}_3 \cap \mathcal{B}_4)$	Total probability rule	$P(B_{123}) = P(\mathcal{B}_1 \cap \mathcal{B}_2 \cap \mathcal{B}_3) - P(B_{1234})$	Probability of breaching event B_{123}
9	Probabilities $P(\mathcal{B}_1 \cap \mathcal{B}_2)$ and $P(\mathcal{B}_1 \cap \mathcal{B}_2 \cap \mathcal{B}_3)$ from Steps 3 and 5	$(\mathcal{B}_1 \cap \mathcal{B}_2) \setminus (\mathcal{B}_1 \cap \mathcal{B}_2 \cap \mathcal{B}_3)$	Total probability rule	$P\left(\mathcal{B}_1 \cap \mathcal{B}_2 \cap \bar{\mathcal{B}}_3\right) = P(\mathcal{B}_1 \cap \mathcal{B}_2) - P(\mathcal{B}_1 \cap \mathcal{B}_2 \cap \mathcal{B}_3) = P(B_{12} \cup B_{124})$	Total probability of all breaching events including breaches at LS_1 and LS_2, but not at LS_3

Table A1
Continued

Step no.	Preliminary knowledge	Breaching events	Adopted tool	Probability calculation	Description
10	Maximum water level at LS_4 from the flood routing simulation of breaching event B_{12}	$\mathcal{B}_4 \mid (\mathcal{B}_1 \cap \mathcal{B}_2 \cap \bar{\mathcal{B}}_3)$	Fragility function of LS_4	$P(\mathcal{B}_4 \mid \mathcal{B}_1 \cap \mathcal{B}_2 \cap \bar{\mathcal{B}}_3) = P_{f(LS_4)}(\eta_{\max,B_{12}})$	Probability of all breaching events including a breach at LS_4 conditional to the occurrence of breaches at LS_1 and LS_2, but not at LS_3
11	Probabilities $P(\mathcal{B}_1 \cap \mathcal{B}_2 \cap \bar{\mathcal{B}}_3)$ and $P(\mathcal{B}_4 \mid \mathcal{B}_1 \cap \mathcal{B}_2 \cap \bar{\mathcal{B}}_3)$ from Steps 9 and 10	$\mathcal{B}_1 \cap \mathcal{B}_2 \cap \bar{\mathcal{B}}_3 \cap \mathcal{B}_4$	Probability multiplication rule for dependent events	$P(\mathcal{B}_1 \cap \mathcal{B}_2 \cap \bar{\mathcal{B}}_3 \cap \mathcal{B}_4) = P(\mathcal{B}_1 \cap \mathcal{B}_2 \cap \bar{\mathcal{B}}_3) \cdot P(\mathcal{B}_4 \mid \mathcal{B}_1 \cap \mathcal{B}_2 \cap \bar{\mathcal{B}}_3) = P(B_{124})$	Probability of breaching event B_{124}
12	Probabilities $P(\mathcal{B}_1 \cap \mathcal{B}_2 \cap \bar{\mathcal{B}}_3)$ and $P(\mathcal{B}_1 \cap \mathcal{B}_2 \cap \bar{\mathcal{B}}_3 \cap \mathcal{B}_4)$ from Steps 9 and 11	$(\mathcal{B}_1 \cap \mathcal{B}_2 \cap \bar{\mathcal{B}}_3)$ $(\mathcal{B}_1 \cap \mathcal{B}_2 \cap \bar{\mathcal{B}}_3 \cap \mathcal{B}_4)$	Total probability rule	$P(\mathcal{B}_1 \cap \mathcal{B}_2 \cap \bar{\mathcal{B}}_3 \cap \bar{\mathcal{B}}_4) = P(\mathcal{B}_1 \cap \mathcal{B}_2 \cap \bar{\mathcal{B}}_3) - P(\mathcal{B}_1 \cap \mathcal{B}_2 \cap \bar{\mathcal{B}}_3 \cap \mathcal{B}_4) = P(B_{12})$	Probability of breaching event B_{12}
13	Probabilities $P(\mathcal{B}_1)$ and $P(\mathcal{B}_1 \cap \mathcal{B}_2)$ from Steps 1 and 3	$\mathcal{B}_1 \cap \bar{\mathcal{B}}_2$	Total probability rule	$P(\mathcal{B}_1 \cap \bar{\mathcal{B}}_2) = P(\mathcal{B}_1) - P(\mathcal{B}_1 \cap \mathcal{B}_2) = P(B_1 \cup B_{13} \cup B_{14} \cup B_{134})$	Total probability of all breaching events including breaches at LS_1, but not at LS_2
14	Maximum water level at LS_3 from the flood routing simulation of breaching event B_1	$\mathcal{B}_3 \mid (\mathcal{B}_1 \cap \bar{\mathcal{B}}_2)$	Fragility function of LS_3	$P(\mathcal{B}_3 \mid \mathcal{B}_1 \cap \bar{\mathcal{B}}_2) = P_{f(LS_3)}(\eta_{\max,B_1})$	Probability of all breaching events including a breach at LS_3 conditional to the occurrence of a breach at LS_1 but not at LS_2
15	Probabilities $P(\mathcal{B}_1 \cap \bar{\mathcal{B}}_2)$ and $P(\mathcal{B}_3 \mid \mathcal{B}_1 \cap \bar{\mathcal{B}}_2)$ from Steps 13 and 14	$\mathcal{B}_1 \cap \bar{\mathcal{B}}_2 \cap \mathcal{B}_3$	Probability multiplication rule for dependent events	$P(\mathcal{B}_1 \cap \bar{\mathcal{B}}_2 \cap \mathcal{B}_3) = P(\mathcal{B}_1 \cap \bar{\mathcal{B}}_2) \cdot P(\mathcal{B}_3 \mid \mathcal{B}_1 \cap \bar{\mathcal{B}}_2) = P(B_{13} \cup B_{134})$	Total probability of all breaching events including breaches at LS_1 and LS_3, but not at LS_2
16	Maximum water level at LS_4 from the flood routing simulation of breaching event B_{13}	$\mathcal{B}_4 \mid (\mathcal{B}_1 \cap \bar{\mathcal{B}}_2 \cap \mathcal{B}_3)$	Fragility function of LS_4	$P(\mathcal{B}_4 \mid \mathcal{B}_1 \cap \bar{\mathcal{B}}_2 \cap \mathcal{B}_3) = P_{f(LS_4)}(\eta_{\max,B_{13}})$	Probability of all breaching events including a breach at LS_4 conditional to the occurrence of a breach at LS_1 and LS_3, but not at LS_2
17	Probabilities $P(\mathcal{B}_1 \cap \bar{\mathcal{B}}_2 \cap \mathcal{B}_3)$ and $P(\mathcal{B}_4 \mid \mathcal{B}_1 \cap \bar{\mathcal{B}}_2 \cap \mathcal{B}_3)$ from Steps 15 and 16	$\mathcal{B}_1 \cap \bar{\mathcal{B}}_2 \cap \mathcal{B}_3 \cap \mathcal{B}_4$	Probability multiplication rule for dependent events	$P(\mathcal{B}_1 \cap \bar{\mathcal{B}}_2 \cap \mathcal{B}_3 \cap \mathcal{B}_4) = P(\mathcal{B}_1 \cap \bar{\mathcal{B}}_2 \cap \mathcal{B}_3) \cdot P(\mathcal{B}_4 \mid \mathcal{B}_1 \cap \bar{\mathcal{B}}_2 \cap \mathcal{B}_3) = P(B_{134})$	Probability of breaching event B_{134}
18	Probabilities $P(\mathcal{B}_1 \cap \bar{\mathcal{B}}_2 \cap \mathcal{B}_3)$ and $P(\mathcal{B}_1 \cap \bar{\mathcal{B}}_2 \cap \mathcal{B}_3 \cap \mathcal{B}_4)$ from Steps 15 and 17	$(\mathcal{B}_1 \cap \bar{\mathcal{B}}_2 \cap \mathcal{B}_3) \setminus (\mathcal{B}_1 \cap \bar{\mathcal{B}}_2 \cap \mathcal{B}_3 \cap \mathcal{B}_4)$	Total probability rule	$P(\mathcal{B}_1 \cap \bar{\mathcal{B}}_2 \cap \mathcal{B}_3) - P(\mathcal{B}_1 \cap \bar{\mathcal{B}}_2 \cap \mathcal{B}_3 \cap \mathcal{B}_4) = P(B_{13})$	Probability of breaching event B_{13}
19	Probabilities $P(\mathcal{B}_1 \cap \bar{\mathcal{B}}_2)$ and $P(\mathcal{B}_1 \cap \bar{\mathcal{B}}_2 \cap \mathcal{B}_3)$ from Steps 13 and 15	$\mathcal{B}_1 \cap \bar{\mathcal{B}}_2 \cap \bar{\mathcal{B}}_3$	Total probability rule	$P(\mathcal{B}_1 \cap \bar{\mathcal{B}}_2 \cap \bar{\mathcal{B}}_3) = P(\mathcal{B}_1 \cap \bar{\mathcal{B}}_2) - P(\mathcal{B}_1 \cap \bar{\mathcal{B}}_2 \cap \mathcal{B}_3) = P(B_1 \cup B_{14})$	Total probability of all breaching events including breaches at LS_1 but not at LS_2 and LS_3

Table A1
Continued

Step no.	Preliminary knowledge	Breaching events	Adopted tool	Probability calculation	Description
20	Maximum water level at LS_4 from the flood routing simulation of breaching event B_1	$\mathcal{B}_4 \mid (\mathcal{B}_1 \cap \bar{\mathcal{B}}_2 \cap \bar{\mathcal{B}}_3)$	Fragility function of LS_4	$P(\mathcal{B}_4 \mid \mathcal{B}_1 \cap \bar{\mathcal{B}}_2 \cap \bar{\mathcal{B}}_3) = P_{f(LS_4)}(\eta_{\max,B_1})$	Probability of all breaching events including a breach at LS_4 conditional to the occurrence of a breach at LS_1 but not at LS_2 and LS_3
21	Probabilities $P(\mathcal{B}_1 \cap \bar{\mathcal{B}}_2 \cap \bar{\mathcal{B}}_3)$ and $P(\mathcal{B}_4 \mid \mathcal{B}_1 \cap \bar{\mathcal{B}}_2 \cap \bar{\mathcal{B}}_3)$ from Steps 19 and 20	$\mathcal{B}_1 \cap \bar{\mathcal{B}}_2 \cap \bar{\mathcal{B}}_3 \cap \mathcal{B}_4$	Probability multiplication rule for dependent events	$P(\mathcal{B}_1 \cap \bar{\mathcal{B}}_2 \cap \bar{\mathcal{B}}_3 \cap \mathcal{B}_4) = P(\mathcal{B}_1 \cap \bar{\mathcal{B}}_2 \cap \bar{\mathcal{B}}_3) \cdot P(\mathcal{B}_4 \mid \mathcal{B}_1 \cap \bar{\mathcal{B}}_2 \cap \bar{\mathcal{B}}_3) = P(B_{14})$	Probability of breaching event B_{14}
22	Probabilities $P(\mathcal{B}_1 \cap \bar{\mathcal{B}}_2 \cap \bar{\mathcal{B}}_3)$ and $P(\mathcal{B}_1 \cap \bar{\mathcal{B}}_2 \cap \bar{\mathcal{B}}_3 \cap \mathcal{B}_4)$ from Steps 19 and 21	$\mathcal{B}_1 \cap \bar{\mathcal{B}}_2 \cap \bar{\mathcal{B}}_3 \cap \bar{\mathcal{B}}_4$	Total probability rule	$P(\mathcal{B}_1 \cap \bar{\mathcal{B}}_2 \cap \bar{\mathcal{B}}_3 \cap \bar{\mathcal{B}}_4) = P(\mathcal{B}_1 \cap \bar{\mathcal{B}}_2 \cap \bar{\mathcal{B}}_3) - P(\mathcal{B}_1 \cap \bar{\mathcal{B}}_2 \cap \bar{\mathcal{B}}_3 \cap \mathcal{B}_4) = P(B_1)$	Probability of breaching event B_1
23	Maximum water level at LS_2 from the preliminary flood routing simulation	$\mathcal{B}_2 \mid \bar{\mathcal{B}}_1$	Fragility function of LS_2	$P(\mathcal{B}_2 \mid \bar{\mathcal{B}}_1) = P_{f(LS_2)}(\eta_{\max,B_0})$	Probability of all breaching events including a breach at LS_2 conditional to the fact that a breach has not occurred at LS_1
24	Probabilities $P(\bar{\mathcal{B}}_1)$ and $P(\mathcal{B}_2 \mid \bar{\mathcal{B}}_1)$ from Steps 1 and 23	$\mathcal{B}_2 \cap \bar{\mathcal{B}}_1$	Probability multiplication rule for dependent events	$P(\mathcal{B}_2 \cap \bar{\mathcal{B}}_1) = [1 - P(\mathcal{B}_1)] \cdot P(\mathcal{B}_2 \mid \bar{\mathcal{B}}_1) = P(B_2 \cup B_{23} \cup B_{24} \cup B_{234})$	Total probability of all breaching events including breaches at LS_2 and not at LS_1
25	Maximum water level at LS_3 from the flood routing simulation of breaching event B_2	$\mathcal{B}_3 \mid (\mathcal{B}_2 \cap \bar{\mathcal{B}}_1)$	Fragility function of LS_3	$P(\mathcal{B}_3 \mid \mathcal{B}_2 \cap \bar{\mathcal{B}}_1) = P_{f(LS_3)}(\eta_{\max,B_2})$	Probability of all breaching events including a breach at LS_3 conditional to the occurrence of a breach at LS_2, but not at LS_1
26	Probabilities $P(\mathcal{B}_2 \cap \bar{\mathcal{B}}_1)$ and $P(\mathcal{B}_3 \mid \mathcal{B}_2 \cap \bar{\mathcal{B}}_1)$ from Steps 24 and 25	$\mathcal{B}_2 \cap \mathcal{B}_3 \cap \bar{\mathcal{B}}_1$	Probability multiplication rule for dependent events	$P(\mathcal{B}_2 \cap \mathcal{B}_3 \cap \bar{\mathcal{B}}_1) = P(\mathcal{B}_2 \cap \bar{\mathcal{B}}_1) \cdot P(\mathcal{B}_3 \mid \mathcal{B}_2 \cap \bar{\mathcal{B}}_1) = P(B_{23} \cup B_{234})$	Total probability of all breaching events including breaches at LS_2 and LS_3, but not at LS_1
27	Maximum water level at LS_4 from the flood routing simulation of breaching event B_{23}	$\mathcal{B}_4 \mid (\mathcal{B}_2 \cap \mathcal{B}_3 \cap \bar{\mathcal{B}}_1)$	Fragility function of LS_4	$P(\mathcal{B}_4 \mid \mathcal{B}_2 \cap \mathcal{B}_3 \cap \bar{\mathcal{B}}_1) = P_{f(LS_4)}(\eta_{\max,B_{23}})$	Probability of all breaching events including a breach at LS_4 conditional to the occurrence of breaches at LS_2 and LS_3, but not at LS_1
28	Probabilities $P(\mathcal{B}_2 \cap \mathcal{B}_3 \cap \bar{\mathcal{B}}_1)$ and $P(\mathcal{B}_4 \mid \mathcal{B}_2 \cap \mathcal{B}_3 \cap \bar{\mathcal{B}}_1)$ from Steps 26 and 27	$\mathcal{B}_2 \cap \mathcal{B}_3 \cap \mathcal{B}_4 \cap \bar{\mathcal{B}}_1$	Probability multiplication rule for dependent events	$P(\mathcal{B}_2 \cap \mathcal{B}_3 \cap \mathcal{B}_4 \cap \bar{\mathcal{B}}_1) = P(\mathcal{B}_2 \cap \mathcal{B}_3 \cap \bar{\mathcal{B}}_1) \cdot P(\mathcal{B}_4 \mid \mathcal{B}_2 \cap \mathcal{B}_3 \cap \bar{\mathcal{B}}_1) = P(B_{234})$	Probability of breaching event B_{234}
29	Probabilities $P(\mathcal{B}_2 \cap \mathcal{B}_3 \cap \bar{\mathcal{B}}_1)$ and $P(\mathcal{B}_2 \cap \mathcal{B}_3 \cap \mathcal{B}_4 \cap \bar{\mathcal{B}}_1)$ from Steps 26 and 28	$(\mathcal{B}_2 \cap \mathcal{B}_3 \cap \bar{\mathcal{B}}_1) \setminus (\mathcal{B}_2 \cap \mathcal{B}_3 \cap \mathcal{B}_4 \cap \bar{\mathcal{B}}_1)$	Total probability rule	$P(\mathcal{B}_2 \cap \mathcal{B}_3 \cap \bar{\mathcal{B}}_1) - P(\mathcal{B}_2 \cap \mathrm{B}_3 \cap \mathrm{B}_4 \cap \bar{\mathcal{B}}_1) = P(B_{23})$	Probability of breaching event B_{23}

Table A1
Continued

Step no.	Preliminary knowledge	Breaching events	Adopted tool	Probability calculation	Description
30	Probabilities $P\left(\mathcal{B}_2 \cap \bar{\mathcal{B}}_1\right)$ and $P\left(\mathcal{B}_2 \cap \mathcal{B}_3 \cap \bar{\mathcal{B}}_1\right)$ from Steps 24 and 26	$\mathcal{B}_2 \cap \bar{\mathcal{B}}_1 \cap \bar{\mathcal{B}}_3$	Total probability rule	$P\left(\mathcal{B}_2 \cap \bar{\mathcal{B}}_1 \cap \bar{\mathcal{B}}_3\right) = P\left(\mathcal{B}_2 \cap \bar{\mathcal{B}}_1\right) - P\left(\mathcal{B}_2 \cap \mathcal{B}_3 \cap \bar{\mathcal{B}}_1\right) = P\left(B_{24} \cup B_2\right)$	Total probability of all breaching events including breaches at LS_2 but not at LS_1 and LS_3
31	Maximum water level at LS_4 from the flood routing simulation of breaching event B_2	$\mathcal{B}_4 \mid \left(\mathcal{B}_2 \cap \bar{\mathcal{B}}_1 \cap \bar{\mathcal{B}}_3\right)$	Fragility function of LS_4	$P\left(\mathcal{B}_4 \mid \mathcal{B}_2 \cap \bar{\mathcal{B}}_1 \cap \bar{\mathcal{B}}_3\right) = P_{f\left(LS_4\right)}\left(\eta_{\max,B_2}\right)$	Probability of all breaching events including a breach at LS_4 conditional to the occurrence of a breach at LS_2 but not at LS_1 and LS_3
32	Probabilities $P\left(\mathcal{B}_2 \cap \bar{\mathcal{B}}_1 \cap \bar{\mathcal{B}}_3\right)$ and $P\left(\mathcal{B}_4 \mid \mathcal{B}_2 \cap \bar{\mathcal{B}}_1 \cap \bar{\mathcal{B}}_3\right)$ from Steps 30 and 31	$\mathcal{B}_2 \cap \mathcal{B}_4 \cap \bar{\mathcal{B}}_1 \cap \bar{\mathcal{B}}_3$	Probability multiplication rule for dependent events	$P\left(\mathcal{B}_2 \cap \mathcal{B}_4 \cap \bar{\mathcal{B}}_1 \cap \bar{\mathcal{B}}_3\right) = P\left(\mathcal{B}_2 \cap \bar{\mathcal{B}}_1 \cap \bar{\mathcal{B}}_3\right) \cdot P\left(\mathcal{B}_4 \mid \mathcal{B}_2 \cap \bar{\mathcal{B}}_1 \cap \bar{\mathcal{B}}_3\right) = P\left(B_{24}\right)$	Probability of breaching event B_{24}
33	Probabilities $P\left(\mathcal{B}_2 \cap \bar{\mathcal{B}}_1 \cap \bar{\mathcal{B}}_3\right)$ and $P\left(\mathcal{B}_2 \cap \mathcal{B}_4 \cap \bar{\mathcal{B}}_1 \cap \bar{\mathcal{B}}_3\right)$ from Steps 30 and 32	$\left(\mathcal{B}_2 \cap \bar{\mathcal{B}}_1 \cap \bar{\mathcal{B}}_3\right) \setminus \left(\mathcal{B}_2 \cap \mathcal{B}_4 \cap \bar{\mathcal{B}}_1 \cap \bar{\mathcal{B}}_3\right)$	Total probability rule	$P\left(\mathcal{B}_2 \cap \bar{\mathcal{B}}_1 \cap \bar{\mathcal{B}}_3\right) - P\left(\mathcal{B}_2 \cap \mathcal{B}_4 \cap \bar{\mathcal{B}}_1 \cap \bar{\mathcal{B}}_3\right) = P\left(B_2\right)$	Probability of breaching event B_2
34	Maximum water level at LS_3 from the preliminary flood routing simulation	$\mathcal{B}_3 \mid \left(\bar{\mathcal{B}}_1 \cap \bar{\mathcal{B}}_2\right)$	Fragility function of LS_3	$P\left(\mathcal{B}_3 \mid \bar{\mathcal{B}}_1 \cap \bar{\mathcal{B}}_2\right) = P_{f\left(LS_3\right)}\left(\eta_{\max,B_0}\right)$	Probability of all breaching events including a breach at LS_3 conditional to the fact that a breach has not occurred at LS_1 and LS_2
35	Probabilities $P\left(\bar{\mathcal{B}}_1 \cap \bar{\mathcal{B}}_2\right)$ and $P\left(\mathcal{B}_3 \mid \bar{\mathcal{B}}_1 \cap \bar{\mathcal{B}}_2\right)$ from Steps 1, 24, and 34	$\mathcal{B}_3 \cap \bar{\mathcal{B}}_1 \cap \bar{\mathcal{B}}_2$	Probability multiplication rule for dependent events	$P\left(\mathcal{B}_3 \cap \bar{\mathcal{B}}_1 \cap \bar{\mathcal{B}}_2\right) = P\left(\bar{\mathcal{B}}_1 \cap \bar{\mathcal{B}}_2\right) \cdot P\left(\mathcal{B}_3 \mid \bar{\mathcal{B}}_1 \cap \bar{\mathcal{B}}_2\right) = \left[1 - P\left(\mathcal{B}_1\right) - P\left(\mathcal{B}_2 \cap \bar{\mathcal{B}}_1\right)\right] \cdot P\left(\mathcal{B}_3 \mid \bar{\mathcal{B}}_1 \cap \bar{\mathcal{B}}_2\right) = P\left(B_3 \cup B_{34}\right)$	Total probability of all breaching events including breaches at LS_3 and not at LS_1 and LS_2
36	Maximum water level at LS_4 from the flood routing simulation of breaching event B_3	$\mathcal{B}_4 \mid \left(\mathcal{B}_3 \cap \bar{\mathcal{B}}_1 \cap \bar{\mathcal{B}}_2\right)$	Fragility function of LS_4	$P\left(\mathcal{B}_4 \mid \mathcal{B}_3 \cap \bar{\mathcal{B}}_1 \cap \bar{\mathcal{B}}_2\right) = P_{f\left(LS_4\right)}\left(\eta_{\max,B_3}\right)$	Probability of all breaching events including a breach at LS_4 conditional to the occurrence of a breach at LS_3 but not at LS_1 and LS_2
37	Probabilities $P\left(\mathcal{B}_3 \cap \bar{\mathcal{B}}1 \cap \bar{\mathcal{B}}_2\right)$ and $P\left(\mathcal{B}_4 \mid \mathcal{B}_3 \cap \bar{\mathcal{B}}_1 \cap \bar{\mathcal{B}}_2\right)$ from Steps 35 and 36	$\mathcal{B}_3 \cap \mathcal{B}_4 \cap \bar{\mathcal{B}}_1 \cap \bar{\mathcal{B}}_2$	Probability multiplication rule for dependent events	$P\left(\mathcal{B}_3 \cap \mathcal{B}_4 \cap \bar{\mathcal{B}}_1 \cap \bar{\mathcal{B}}_2\right) = P\left(\mathcal{B}_3 \cap \bar{\mathcal{B}}_1 \cap \bar{\mathcal{B}}_2\right) \cdot P\left(\mathcal{B}_4 \mid \mathcal{B}_3 \cap \bar{\mathcal{B}}_1 \cap \bar{\mathcal{B}}_2\right) = P\left(B_{34}\right)$	Probability of breaching event B_{34}
38	Probabilities $P\left(\mathcal{B}_3 \cap \bar{\mathcal{B}}1 \cap \bar{\mathcal{B}}_2\right)$ and $P\left(\mathcal{B}_3 \cap \mathcal{B}_4 \cap \bar{\mathcal{B}}_1 \cap \bar{\mathcal{B}}_2\right)$ from Steps 35 and 37	$\left(\mathcal{B}_3 \cap \bar{\mathcal{B}}_1 \cap \bar{\mathcal{B}}_2\right) \setminus \left(\mathcal{B}_3 \cap \mathcal{B}_4 \cap \bar{\mathcal{B}}_1 \cap \bar{\mathcal{B}}_2\right)$	Total probability rule	$P\left(\mathcal{B}_3 \cap \bar{\mathcal{B}}_1 \cap \bar{\mathcal{B}}_2\right) - P\left(\mathcal{B}_3 \cap \mathcal{B}_4 \cap \bar{\mathcal{B}}_1 \cap \bar{\mathcal{B}}_2\right) = P\left(B_3\right)$	Probability of breaching event B_3
39	Maximum water level at LS_4 from the preliminary flood routing simulation	$\mathcal{B}_4 \mid \left(\bar{\mathcal{B}}_1 \cap \bar{\mathcal{B}}_2 \cap \bar{\mathcal{B}}_3\right)$	Fragility function of LS_4	$P\left(\mathcal{B}_4 \mid \bar{\mathcal{B}}_1 \cap \bar{\mathcal{B}}_2 \cap \bar{\mathcal{B}}_3\right) = P_{f\left(LS_4\right)}\left(\eta_{\max,B_0}\right)$	Probability of all breaching events including a breach at LS_4 conditional to the fact that a breach has not occurred at LS_1, LS_2, and LS_3

Table A1
Continued

Step no.	Preliminary knowledge	Breaching events	Adopted tool	Probability calculation	Description
40	Probabilities $P\left(\bar{\mathcal{B}}_1 \cap \bar{\mathcal{B}}_2 \cap \bar{\mathcal{B}}_3\right)$ and $P\left(\mathcal{B}_4 \mid \bar{\mathcal{B}}_1 \cap \bar{\mathcal{B}}_2 \cap \bar{\mathcal{B}}_3\right)$ from Steps 1, 24, 35, and 39	$\mathcal{B}_4 \cap \bar{\mathcal{B}}_1 \cap \bar{\mathcal{B}}_2 \cap \bar{\mathcal{B}}_3$	Probability multiplication rule for dependent events	$P\left(\mathcal{B}_4 \cap \bar{\mathcal{B}}_1 \cap \bar{\mathcal{B}}_2 \cap \bar{\mathcal{B}}_3\right) = P\left(\bar{\mathcal{B}}_1 \cap \bar{\mathcal{B}}_2 \cap \bar{\mathcal{B}}_3\right) \cdot P\left(\mathcal{B}_4 \mid \bar{\mathcal{B}}_1 \cap \bar{\mathcal{B}}_2 \cap \bar{\mathcal{B}}_3\right) = \left[1 - P\left(\mathcal{B}_1\right) - P\left(\mathcal{B}_2 \cap \bar{\mathcal{B}}_1\right) - P\left(\mathcal{B}_3 \cap \bar{\mathcal{B}}_1 \cap \bar{\mathcal{B}}_2\right)\right] \cdot P\left(\mathcal{B}_4 \mid \bar{\mathcal{B}}_1 \cap \bar{\mathcal{B}}_2 \cap \bar{\mathcal{B}}_3\right) = P\left(B_4\right)$	Probability of breaching event B_4
41	Probabilities from Steps 1, 24, 35, and 40	B_0	Total probability rule	$P\left(B_0\right) = 1 - P\left(\mathcal{B}_1\right) - P\left(\mathcal{B}_2 \cap \bar{\mathcal{B}}_1\right) - P\left(\mathcal{B}_3 \cap \bar{\mathcal{B}}_1 \cap \bar{\mathcal{B}}_2\right) - P\left(\mathcal{B}_4 \cap \bar{\mathcal{B}}_1 \cap \bar{\mathcal{B}}_2 \cap \bar{\mathcal{B}}_3\right)$	Probability of no breach event B_0

Note. The table is ideally divided in five sections: the first section (Steps 1–22) refers to the calculation of probabilities of breaching events belonging to space $\mathcal{B}_1$; the second section (Steps 23–33) refers to space $\mathcal{B}_2 \cap \bar{\mathcal{B}}_1$; the third section (Steps 34–38) refers to space $\mathcal{B}_3 \cap \bar{\mathcal{B}}_2 \cap \bar{\mathcal{B}}_1$; the fourth section (Steps 39–40) refers to space $\mathcal{B}_4 \cap \bar{\mathcal{B}}_3 \cap \bar{\mathcal{B}}_2 \cap \bar{\mathcal{B}}_1$; and the last section (Step 41) refers to no breach event B_0.

Data Availability Statement

The cross-sectional data of the Po River are available on the Italian Interregional Agency for the Po River (AIPo) website at http://geoportale.agenziapo.it/web/index.php/it/. The topographic data of the flood prone area can be accessed on the National Geoportal of the Italian Ministry of Environment and Protection of Land and Sea website at http://www.pcn.minambiente.it/mattm/en/data-distribution-service-pst/. All data used in this paper can be accessed in a public repository at https://doi.org/10.6084/m9.figshare.15016371.

Acknowledgments
The Editor (J. Hall), the Associate Editor, and the two anonymous reviewers are kindly acknowledged for their valuable suggestions and comments, which have contributed to the improvement of the paper. Open Access Funding provided by University of Parma (Italy) within the CRUI-CARE Agreement.

References

ACER Technical Memorandum No. 11. (1988). *Downstream hazard classification guidelines*. U.S. Department of the Interior, Bureau of Reclamation.

Akhter, F., Mazzoleni, M., & Brandimarte, L. (2021). Analysis of 220 years of floodplain population dynamics in the US at different spatial scales. *Water*, *13*(2), 141. https://doi.org/10.3390/w13020141

Alonso Vicario, S., Mazzoleni, M., Bhamidipati, S., Gharesifard, M., Ridolfi, E., Pandolfo, C., & Alfonso, L. (2020). Unravelling the influence of human behaviour on reducing casualties during flood evacuation. *Hydrological Sciences Journal*, *65*(14), 2359–2375. https://doi.org/10.1080/02626667.2020.1810254

Apel, H., Merz, B., & Thieken, A. H. (2009). Influence of dike breaches on flood frequency estimation. *Computers & Geosciences*, *35*(5), 907–923. https://doi.org/10.1016/j.cageo.2007.11.003

Apel, H., Thieken, A. H., Merz, B., & Blöschl, G. (2006). A Probabilistic modelling system for assessing flood risks. *Natural Hazards*, *38*(1–2), 79–100. https://doi.org/10.1007/s11069-005-8603-7

Aronica, G. T., Candela, A., Fabio, P., & Santoro, M. (2012). Estimation of flood inundation probabilities using global hazard indexes based on hydrodynamic variables. *Physics and Chemistry of the Earth, Parts A/B/C*, *42–44*, 119–129. https://doi.org/10.1016/j.pce.2011.04.001

Aureli, A., Maranzoni, A., Mignosa, P., & Ziveri, C. (2006). Flood hazard mapping by means of fully-2D and quasi-2D numerical modeling: A case study. *Paper presented at 3rd International Symposium on Flood Defence*. Taylor & Francis.

Aureli, F., & Mignosa, P. (2004). Flooding scenarios due to levee breaking in the Po river. *Proceedings of the Institution of Civil Engineers - Water Management*, *157*(1), 3–12. https://doi.org/10.1680/wama.2004.157.1.3

Beven, K., Lamb, R., Leedal, D., & Hunter, N. (2015). Communicating uncertainty in flood inundation mapping: A case study. *International Journal of River Basin Management*, *13*(3), 285–295. https://doi.org/10.1080/15715124.2014.917318

Blöschl, G., Hall, J., Viglione, A., Perdigão, R. A. P., Parajka, J., Merz, B., et al. (2019). Changing climate both increases and decreases European river floods. *Nature*, *573*(7772), 108–111. https://doi.org/10.1038/s41586-019-1495-6

Bodi, L., Nagy, L., & Takacs, A. (2014). Review of historic floods in Hungary and the extent of flooded areas in case of levee failures. In *6th Canadian Geohazards Conference*. The Canadian Geotechnical Society.

Bomers, A., Schielen, R. M. J., & Hulscher, S. J. M. H. (2019). Consequences of dike breaches and dike overflow in a bifurcating river system. *Natural Hazards*, *97*(1), 309–334. https://doi.org/10.1007/s11069-019-03643-y

Brunner, G. W. (2016a). *HEC-RAS, River Analysis System, 2D modeling user's manual Version 5.0*. U.S. Army Corps of Engineers, Institute for Water Resources, Hydrologic Engineering Center.

Brunner, G. W. (2016b). *HEC-RAS, River Analysis System, hydraulic reference manual*. U.S. Army Corps of Engineers, Institute for Water Resources, Hydrologic Engineering Center.

Butera, I., Climaci, M., & Tanda, M. G. (2020). Numerical analysis of phreatic levels in river embankments due to flood events. *Journal of Hydrology*, *590*, 125382. https://doi.org/10.1016/j.jhydrol.2020.125382

Chow, V. T., Maidment, D. R., & Mays, L. W. (1988). *Applied hydrology*. McGraw-Hill.

Ciullo, A., de Bruijn, K. M., Kwakkel, J. H., & Klijn, F. (2019). Accounting for the uncertain effects of hydraulic interactions in optimising embankments heights: Proof of principle for the IJssel River. *Journal of Flood Risk Management*, *12*(S2), e12532. https://doi.org/10.1111/jfr3.12532

Corine Land Cover. (2012). Retrieved from https://land.copernicus.eu/pan-european/corine-land-cover/clc-2012

Courage, W., Vrouwenvelder, T., van Mierlo, T., & Schweckendiek, T. (2013). System behaviour in flood risk calculations. *Georisk: Assessment and Management of Risk for Engineered Systems and Geohazards*, *7*(2), 62–76. https://doi.org/10.1080/17499518.2013.790732

Curran, A., De Bruijn, K., Domeneghetti, A., Bianchi, F., Kok, M., Vorogushyn, S., & Castellarin, A. (2020). Large-scale stochastic flood hazard analysis applied to the Po River. *Natural Hazards*, *104*(3), 2027–2049. https://doi.org/10.1007/s11069-020-04260-w

Curran, A., De Bruijn, K. M., & Kok, M. (2020). Influence of water level duration on dike breach triggering, focusing on system behaviour hazard analyses in lowland rivers. *Georisk: Assessment and Management of Risk for Engineered Systems and Geohazards*, *14*(1), 26–40. https://doi.org/10.1080/17499518.2018.1542498

Dawson, R., & Hall, J. (2006). Adaptive importance sampling for risk analysis of complex infrastructure systems. *Proceedings of the Royal Society A: Mathematical, Physical & Engineering Sciences*, *462*(2075), 3343–3362. https://doi.org/10.1098/rspa.2006.1720

Dawson, R., Hall, J., Sayers, P., Bates, P., & Rosu, C. (2005). Sampling-based flood risk analysis for fluvial dike systems. *Stochastic Environmental Research and Risk Assessment*, *19*(6), 388–402. https://doi.org/10.1007/s00477-005-0010-9

de Bruijn, K. M. (2004). Resilience indicators for flood risk management systems of lowland rivers. *International Journal of River Basin Management*, *2*(3), 199–210. https://doi.org/10.1080/15715124.2004.9635232

DEFRA Environment Agency. (2006). *Flood Risks to people (FD2321/TR2 guidance document)*. U.K. Department for Environment, Food and Rural Affairs.

de Moel, H., van Alphen, J., & Aerts, J. C. J. H. (2009). Flood maps in Europe–methods, availability and use. *Natural Hazards and Earth System Sciences*, *9*(2), 289–301. https://doi.org/10.5194/nhess-9-289-2009

Di Baldassarre, G., Castellarin, A., Montanari, A., & Brath, A. (2009). Probability-weighted hazard maps for comparing different flood risk management strategies: A case study. *Natural Hazards*, *50*(3), 479–496. https://doi.org/10.1007/s11069-009-9355-6

Di Baldassarre, G., Kreibich, H., Vorogushyn, S., Aerts, J., Arnbjerg-Nielsen, K., Barendrecht, M., et al. (2018). Hess opinions: An interdisciplinary research agenda to explore the unintended consequences of structural flood protection. *Hydrology and Earth System Sciences*, *22*(11), 5629–5637. https://doi.org/10.5194/hess-22-5629-2018

Di Baldassarre, G., Schumann, G., Bates, P. D., Freer, J. E., & Beven, K. J. (2010). Flood-plain mapping: A critical discussion of deterministic and probabilistic approaches. *Hydrological Sciences Journal*, *55*(3), 364–376. https://doi.org/10.1080/02626661003683389

Dierauer, J., Pinter, N., & Remo, J. W. F. (2012). Evaluation of levee setbacks for flood-loss reduction, Middle Mississippi River, USA. *Journal of Hydrology*, *450–451*, 1–8. https://doi.org/10.1016/j.jhydrol.2012.05.044

D'Oria, M., Maranzoni, A., & Mazzoleni, M. (2019). Probabilistic assessment of flood hazard due to levee breaches using fragility functions. *Water Resources Research*, *55*(11), 8740–8764. https://doi.org/10.1029/2019WR025369

Dottori, F., Di Baldassarre, G., & Todini, E. (2013). Detailed data is welcome, but with a pinch of salt: Accuracy, precision, and uncertainty in flood inundation modeling. *Water Resources Research*, *49*(9), 6079–6085. https://doi.org/10.1002/wrcr.20406

EXCIMAP. (2007). In J. van Alphen & R. Passchier (Eds.), *Atlas of flood maps: Examples from 19 European countries, USA and Japan*. Ministry of Transport, Public Works and Water Management, The Netherlands.

Fang, Q. (2016). Adapting Chinese cities to climate change. *Science*, *354*(6311), 425–426. https://doi.org/10.1126/science.aak9826

FEMA. (2013). *Federal guidelines for inundation mapping of flood risk associated with dam incidents and failures (FEMA P-946)*. U.S. Department of Homeland Security.

FEMA. (2020). *Guidance for flood risk analysis and mapping, flood risk assessments*. U.S. Department of Homeland Security.

Ferdous, M. R., Wesselink, A., Brandimarte, L., Slager, K., Zwarteveen, M., & Di Baldassarre, G. (2019). The costs of living with floods in the Jamuna floodplain in Bangladesh. *Water*, *11*(6), 1238. https://doi.org/10.3390/w11061238

Ferrari, A., Dazzi, S., Vacondio, R., & Mignosa, P. (2020). Enhancing the resilience to flooding induced by levee breaches in lowland areas: A methodology based on numerical modelling. *Natural Hazards and Earth System Sciences*, *20*(1), 59–72. https://doi.org/10.5194/nhess-20-59-2020

Feyen, L., Dankers, R., Bódis, K., Salamon, P., & Barredo, J. I. (2012). Fluvial flood risk in Europe in present and future climates. *Climatic Change*, *112*(1), 47–62. https://doi.org/10.1007/s10584-011-0339-7

Garcia, C., & Fearnley, C. J. (2012). Evaluating critical links in early warning systems for natural hazards. *Environmental Hazards*, *11*(2), 123–137. https://doi.org/10.1080/17477891.2011.609877

Hall, J. W., Dawson, R. J., Sayers, P. B., Rosu, C., Chatterton, J. B., & Deakin, R. (2003). A methodology for national-scale flood risk assessment. *Proceedings of the Institution of Civil Engineers - Water and Maritime Engineering*, *156*(3), 235–247. https://doi.org/10.1680/wame.2003.156.3.235

Hall, J. W., Tarantola, S., Bates, P. D., & Horritt, M. S. (2005). Distributed sensitivity analysis of flood inundation model calibration. *Journal of Hydraulic Engineering*, *131*(2), 117–126. https://doi.org/10.1061/(asce)0733-9429(2005)131:2(117)

Harvey, H., Hall, J., & Manning, L. (2014). Computing flood risk in locations protected by flood defences. *Proceedings of the Institution of Civil Engineers - Water Management*, *167*(1), 38–50. https://doi.org/10.1680/wama.12.00106

Hesselink, A. W., Stelling, G. S., Kwadijk, J. C. J., & Middelkoop, H. (2003). Inundation of a Dutch river polder, sensitivity analysis of a physically based inundation model using historic data. *Water Resources Research*, *39*(9), 1234. https://doi.org/10.1029/2002WR001334

Hu, P., Zhang, Q., Shi, P., Chen, B., & Fang, J. (2018). Flood-induced mortality across the globe: Spatiotemporal pattern and influencing factors. *Science of the Total Environment*, *643*, 171–182. https://doi.org/10.1016/j.scitotenv.2018.06.197

Hui, R., Jachens, E., & Lund, J. (2016). Risk-based planning analysis for a single levee. *Water Resources Research*, *52*(4), 2513–2528. https://doi.org/10.1002/2014WR016478

Hutton, N. S., Tobin, G. A., & Montz, B. E. (2019). The levee effect revisited: Processes and policies enabling development in Yuba County, California. *Journal of Flood Risk Management*, *12*(3), e12469. https://doi.org/10.1111/jfr3.12469

Ji, Y., Zhou, G., Wang, S., & Wang, L. (2015). Increase in flood and drought disasters during 1500–2000 in Southwest China. *Natural Hazards*, *77*(3), 1853–1861. https://doi.org/10.1007/s11069-015-1679-9

Jonkman, S. N., Kok, M., & Vrijling, J. K. (2008). Flood risk assessment in the Netherlands: A case study for dike ring South Holland. *Risk Analysis*, *28*(5), 1357–1374. https://doi.org/10.1111/j.1539-6924.2008.01103.x

Karrasch, L., Restemeyer, B., & Klenke, T. (2021). The 'Flood Resilience Rose': A management tool to promote transformation towards flood resilience. *Journal of Flood Risk Management*, e12726. https://doi.org/10.1111/jfr3.12726

Klemešová, K. (2016). Flood maps in the Czech Republic: Content, perception and information value. *E3S Web of Conferences*, 7, 10006. https://doi.org/10.1051/e3sconf/20160710006

Kundzewicz, Z. W., Kanae, S., Seneviratne, S. I., Handmer, J., Nicholls, N., Peduzzi, P., et al. (2014). Flood risk and climate change: Global and regional perspectives. *Hydrological Sciences Journal*, *59*(1), 1–28. https://doi.org/10.1080/02626667.2013.857411

Kvočka, D., Falconer, R. A., & Bray, M. (2016). Flood hazard assessment for extreme flood events. *Natural Hazards*, *84*(3), 1569–1599. https://doi.org/10.1007/s11069-016-2501-z

Maione, U., Mignosa, P., & Tomirotti, M. (2003). Regional estimation of synthetic design hydrographs. *International Journal of River Basin Management*, *1*(2), 151–163. https://doi.org/10.1080/15715124.2003.9635202

Mani, P., Chatterjee, C., & Kumar, R. (2014). Flood hazard assessment with multiparameter approach derived from coupled 1D and 2D hydrodynamic flow model. *Natural Hazards*, *70*(2), 1553–1574. https://doi.org/10.1007/s11069-013-0891-8

Mazzoleni, M., Bacchi, B., Barontini, S., Di Baldassarre, G., Pilotti, M., & Ranzi, R. (2014). Flooding hazard mapping in floodplain areas affected by piping breaches in the Po River, Italy. *Journal of Hydrologic Engineering*, *19*(4), 717–731. https://doi.org/10.1061/(ASCE)HE.1943-5584.0000840

Mazzoleni, M., Barontini, S., Ranzi, R., & Brandimarte, L. (2015). Innovative probabilistic methodology for evaluating the reliability of discrete levee reaches owing to piping. *Journal of Hydrologic Engineering*, *20*(5), 04014067. https://doi.org/10.1061/(ASCE)HE.1943-5584.0001055

Mazzoleni, M., Dottori, F., Brandimarte, L., Tekle, S., & Martina, M. L. V. (2017). Effects of levee cover strength on flood mapping in the case of levee breach due to overtopping. *Hydrological Sciences Journal*, *62*(6), 892–910. https://doi.org/10.1080/02626667.2016.1246800

Mazzoleni, M., Mård, J., Rusca, M., Odongo, V., Lindersson, S., & Di Baldassarre, G. (2021). Floodplains in the Anthropocene: A global analysis of the interplay between human population, built environment and flood severity. *Water Resources Research*, *57*(2), e2020WR027744. https://doi.org/10.1029/2020WR027744

Mel, R. A., Viero, D. P., Carniello, L., & D'Alpaos, L. (2020). Optimal floodgate operation for river flood management: The case study of Padova (Italy). *Journal of Hydrology: Regional Studies*, *30*, 100702. https://doi.org/10.1016/j.ejrh.2020.100702

Merwade, V., Olivera, F., Arabi, M., & Edleman, S. (2008). Uncertainty in flood inundation mapping: Current issues and future directions. *Journal of Hydrologic Engineering*, *13*(7), 608–620. https://doi.org/10.1061/(asce)1084-0699(2008)13:7(608)

Merz, B., Thieken, A. H., & Gocht, M. (2007). Flood risk mapping at the local scale: Concepts and challenges. In *Flood risk management in Europe* (pp. 231–251). Springer. https://doi.org/10.1007/978-1-4020-4200-3_13

Mihu-Pintilie, A., Cîmpianu, C. I., Stoleriu, C. C., Pérez, M. N., & Paveluc, L. E. (2019). Using high-density LiDAR data and 2D streamflow hydraulic modeling to improve urban flood hazard maps: A HEC-RAS multi-scenario approach. *Water*, *11*(9), 1832. https://doi.org/10.3390/w11091832

Mohor, G. S., Hudson, P., & Thieken, A. H. (2020). A comparison of factors driving flood losses in households affected by different flood types. *Water Resources Research*, *56*(4), e2019WR025943. https://doi.org/10.1029/2019WR025943

Most, H. V. D., & Wehrung, M. (2005). Dealing with uncertainty in flood risk assessment of dike rings in the Netherlands. *Natural Hazards*, *36*(1), 191–206. https://doi.org/10.1007/s11069-004-4548-5

Ongdas, N., Akiyanova, F., Karakulov, Y., Muratbayeva, A., & Zinabdin, N. (2020). Application of HEC-RAS (2D) for flood hazard maps generation for Yesil (Ishim) River in Kazakhstan. *Water*, *12*(10), 2672. https://doi.org/10.3390/w12102672

Orlandini, S., Moretti, G., & Albertson, J. D. (2015). Evidence of an emerging levee failure mechanism causing disastrous floods in Italy. *Water Resources Research*, *51*(10), 7995–8011. https://doi.org/10.1002/2015WR017426

Özer, I. E., van Damme, M., & Jonkman, S. N. (2020). Towards an international levee performance database (ILPD) and its use for macro-scale analysis of levee breaches and failures. *Water*, *12*(1), 119. https://doi.org/10.3390/w12010119

Pappenberger, F., Matgen, P., Beven, K. J., Henry, J.-B., Pfister, L., & Fraipont, P. (2006). Influence of uncertain boundary conditions and model structure on flood inundation predictions. *Advances in Water Resources*, *29*(10), 1430–1449. https://doi.org/10.1016/j.advwatres.2005.11.012

Pinter, N. (2005). One step forward, two steps back on U.S. floodplains. *Science*, *308*(5719), 207–208. https://doi.org/10.1126/science.1108411

Pistrika, A. K., & Jonkman, S. N. (2010). Damage to residential buildings due to flooding of New Orleans after hurricane Katrina. *Natural Hazards*, *54*(2), 413–434. https://doi.org/10.1007/s11069-009-9476-y

Sayers, P. B., Hall, J. W., & Meadowcroft, I. C. (2002). Towards risk-based flood hazard management in the UK. *Proceedings of the Institution of Civil Engineers - Civil Engineering*, *150*(5), 36–42. https://doi.org/10.1680/cien.2002.150.5.36

Shannon, C. E. (1948). A mathematical theory of communications. *The Bell System Technical Journal*, *27*(3), 379–423. https://doi.org/10.1002/j.1538-7305.1948.tb01338.x

Shustikova, I., Neal, J. C., Domeneghetti, A., Bates, P. D., Vorogushyn, S., & Castellarin, A. (2020). Levee breaching: A new extension to the LISFLOOD-FP model. *Water*, *12*(4), 942. https://doi.org/10.3390/w12040942

Sills, G. L., Vroman, N. D., Wahl, R. E., & Schwanz, N. T. (2008). Overview of new Orleans levee failures: Lessons learned and their impact on national levee design and assessment. *Journal of Geotechnical and Geoenvironmental Engineering*, *134*(5), 556–565. https://doi.org/10.1061/(asce)1090-0241(2008)134:5(556)

Singh, V. P. (2014). *Entropy theory in hydraulic engineering: An introduction*. American Society of Civil Engineers.

Smemoe, C. M., Nelson, E. J., Zundel, A. K., & Woodruff Miller, A. (2007). Demonstrating floodplain uncertainty using flood probability maps. *Journal of the American Water Resources Association*, *43*(2), 359–371. https://doi.org/10.1111/j.1752-1688.2007.00028.x

Thieken, A. H., Kienzler, S., Kreibich, H., Kuhlicke, C., Kunz, M., Mühr, B., et al. (2016). Review of the flood risk management system in Germany after the major flood in 2013. *Ecology and Society*, *21*(2), 51. https://doi.org/10.5751/ES-08547-210251

Tingsanchali, T., & Karim, M. F. (2005). Flood hazard and risk analysis in the southwest region of Bangladesh. *Hydrological Processes*, *19*(10), 2055–2069. https://doi.org/10.1002/hyp.5666

Turitto, O., Cirio, C. G., Nigrelli, G., Bossuto, P., & Viale, F. (2010). Vulnerabilità manifestata dagli argini maestri del fiume Po negli ultimi due secoli [Vulnerability of main Po River levees in the last 200 years]. *L'Acqua*, *6/2010*, 17–34.

Tyagunov, S., Vorogushyn, S., Muñoz Jimenez, C., Parolai, S., & Fleming, K. (2018). Multi-hazard fragility analysis for fluvial dikes in earthquake- and flood-prone areas. *Natural Hazards and Earth System Sciences*, *18*(9), 2345–2354. https://doi.org/10.5194/nhess-18-2345-2018

Urzică, A., Mihu-Pintilie, A., Stoleriu, C. C., Cîmpianu, C. I., Huţanu, E., Pricop, C. I., & Grozavu, A. (2021). Using 2D HEC-RAS modeling and embankment dam break scenario for assessing the flood control capacity of a multi-reservoir system (NE Romania). *Water*, *13*(1), 57. https://doi.org/10.3390/w13010057

Viero, D. P., D'Alpaos, A., Carniello, L., & Defina, A. (2013). Mathematical modeling of flooding due to river bank failure. *Advances in Water Resources*, *59*, 82–94. https://doi.org/10.1016/j.advwatres.2013.05.011

Viero, D. P., Roder, G., Matticchio, B., Defina, A., & Tarolli, P. (2019). Floods, landscape modifications and population dynamics in anthropogenic coastal lowlands: The Polesine (northern Italy) case study. *Science of the Total Environment*, *651*, 1435–1450. https://doi.org/10.1016/j.scitotenv.2018.09.121

Vorogushyn, S., Apel, H., & Merz, B. (2011). The impact of the uncertainty of dike breach development time on flood hazard. *Physics and Chemistry of the Earth, Parts A/B/C*, *36*(7–8), 319–323. https://doi.org/10.1016/j.pce.2011.01.005

Vorogushyn, S., Merz, B., Lindenschmidt, K.-E., & Apel, H. (2010). A new methodology for flood hazard assessment considering dike breaches. *Water Resources Research*, *46*(8), W08541. https://doi.org/10.1029/2009WR008475

Wahl, T. L. (2004). Uncertainty of predictions of embankment dam breach parameters. *Journal of Hydraulic Engineering*, *130*(5), 389–397. https://doi.org/10.1061/(ASCE)0733-9429(2004)130:5(389)

White, G. F. (1945). *Human adjustment to floods: A geographical approach to the flood problem in the United States*. University of Chicago.

Winter, B., Schneeberger, K., Huttenlau, M., & Stötter, J. (2018). Sources of uncertainty in a probabilistic flood risk model. *Natural Hazards*, *91*(2), 431–446. https://doi.org/10.1007/s11069-017-3135-5